

# Scaling in thermal convection: A unifying theory

Siegfried Grossmann<sup>1</sup> and Detlef Lohse<sup>1,2</sup>

<sup>1</sup> *Fachbereich Physik der Philipps-Universität Marburg,  
Renthof 6, D-35032 Marburg, Germany*

<sup>2</sup> *University of Twente, Department of Applied Physics,  
P.O. Box 217, 7500 AE Enschede, The Netherlands*

(February 5, 2008)

A systematic theory for the scaling of the Nusselt number  $Nu$  and of the Reynolds number  $Re$  in strong Rayleigh-Benard convection is suggested and shown to be compatible with recent experiments. It assumes a coherent large scale convection roll (“wind of turbulence”) and is based on the dynamical equations both in the bulk and in the boundary layers. Several regimes are identified in the Rayleigh number  $Ra$  versus Prandtl number  $Pr$  phase space, defined by whether the boundary layer or the bulk dominates the global kinetic and thermal dissipation, respectively. The crossover between the regimes is calculated. In the regime which has most frequently been studied in experiment ( $Ra \lesssim 10^{11}$ ) the leading terms are  $Nu \sim Ra^{1/4} Pr^{1/8}$ ,  $Re \sim Ra^{1/2} Pr^{-3/4}$  for  $Pr \lesssim 1$  and  $Nu \sim Ra^{1/4} Pr^{-1/12}$ ,  $Re \sim Ra^{1/2} Pr^{-5/6}$  for  $Pr \gtrsim 1$ . In most measurements these laws are modified by additive corrections from the neighboring regimes so that the impression of a slightly larger (effective)  $Nu$  vs  $Ra$  scaling exponent can arise. The most important of the neighboring regimes towards large  $Ra$  are a regime with scaling  $Nu \sim Ra^{1/2} Pr^{1/2}$ ,  $Re \sim Ra^{1/2} Pr^{-1/2}$  for medium  $Pr$  (“Kraichnan regime”), a regime with scaling  $Nu \sim Ra^{1/5} Pr^{1/5}$ ,  $Re \sim Ra^{2/5} Pr^{-3/5}$  for small  $Pr$ , a regime with  $Nu \sim Ra^{1/3}$ ,  $Re \sim Ra^{4/9} Pr^{-2/3}$  for larger  $Pr$ , and a regime with scaling  $Nu \sim Ra^{3/7} Pr^{-1/7}$ ,  $Re \sim Ra^{4/7} Pr^{-6/7}$  for even larger  $Pr$ . In particular, a linear combination of the 1/4 and the 1/3 power laws for  $Nu$  with  $Ra$ ,  $Nu = 0.27Ra^{1/4} + 0.038Ra^{1/3}$  (the prefactors follow from experiment), mimicks a 2/7 power law exponent in a regime as large as ten decades. For very large  $Ra$  the laminar shear boundary layer is speculated to break down through nonnormal-nonlinear transition to turbulence and another regime emerges. – The presented theory is best summarized in the phase diagram figure 1.

## I. INTRODUCTION

The early experiments on turbulent Rayleigh-Benard (RB) convection in air cells with Prandtl number  $Pr \approx 1$ , summarized by Davis [1], showed a power law increase of the Nusselt number  $Nu$  with the Rayleigh number  $Ra$ , namely,  $Nu \sim Ra^\gamma$  with  $\gamma = 1/4$ .<sup>1</sup> However, in these early experiments only relatively small Rayleigh numbers  $Ra \lesssim 10^8$  were achieved. Later, when RB experiments with larger Rayleigh numbers and in water cells with  $Pr \approx 7$  were done, the power law exponent  $\gamma$  turned out to be larger than  $1/4$ . Malkus’ elegant theory of marginal stability, resulting in  $\gamma = 1/3$ , seemed to describe those experiments [2].

In the late 80’s, Libchaber et al.’s experiments done at the University of Chicago on high Rayleigh number Rayleigh-Benard convection in a helium gas cell with Prandtl number  $Pr \approx 1$  revealed new and unexpected scaling for the Nusselt number as a function of the Rayleigh number, namely  $Nu \sim Ra^\gamma$  with  $\gamma = 0.282 \pm 0.006$  [3, 4]. The Reynolds number  $Re$ , characterizing the wind near the walls, i.e., the large eddy mean flow, scaled as  $Re \sim Ra^\alpha$  with  $\alpha = 0.491 \pm 0.002$  [4]. These results were reproduced and extended in many experiments and numerical simulations [5–23]; for review articles, which also summarize the results of earlier experimental, theoretical, and numerical work, we refer to refs. [10, 17, 24]. From all these experiments at first sight it seems that at least the scaling exponent  $\gamma \approx 0.282 \pm 0.006 \approx 2/7$  is very robust.

Various theories were put forward to account for the scaling of the Nusselt number  $Nu$  and the Reynolds number  $Re$  as functions of the Rayleigh number  $Ra$  and the Prandtl number  $Pr$ . These include the Chicago mixing zone model [4] and the Shraiman-Siggia theory [25], both reviewed in refs. [10, 17, 24]. The main result of the Chicago model is  $Nu \sim Ra^{2/7}$ . The Chicago group did not focus on the  $Pr$  dependence as only experiments with  $Pr \approx 1$  were done [4]. Later, Cioni et al. [17] added the  $Pr$  dependence in the spirit of the Chicago model and obtained

$$Nu \sim Ra^{2/7} Pr^{2/7}, \quad (1)$$

$$Re_{fluct} \sim Ra^{3/7} Pr^{-4/7}. \quad (2)$$

Here,  $Re_{fluct}$  refers to the velocity *fluctuations* and not to the large scale mean velocity (often denoted as the “wind of turbulence”) as  $Re$  does. This Prandtl number dependence is only expected to hold for  $Pr < 1$  [17, 24]. On the other hand, the Shraiman-Siggia model, which assumes a turbulent boundary layer (BL) and a thermal boundary layer nested therein (i.e., Shraiman and Siggia implicitly assume a large enough Prandtl number), states

$$Nu \sim Ra^{2/7} Pr^{-1/7}, \quad (3)$$

$$Re \sim Ra^{3/7} Pr^{-5/7} \quad \text{with logarithmic corrections.} \quad (4)$$

For an extension of the Shraiman-Siggia theory to position dependent shear rates see ref. [26]. The Prandtl number dependence of the Nusselt number resulting from the Chicago

---

<sup>1</sup> With the symbol “ $\sim$ ” we mean “scales as” throughout the text, *not* “order of magnitude”. The prefactors are determined in section IV.

model [4] and from the Shraiman-Siggia theory [25] are not contradictory, as eq. (1) has been suggested for small  $Pr$  number fluids and eq. (3) for the large  $Pr$  number case. Indeed, in the large  $Pr$ -limit Zaleski [24] derives the same  $Pr$ -dependence eq. (3) as in the Shraiman-Siggia theory also from the Chicago model. However, both theories are based on rather different assumptions.

In recent years, the Prandtl number dependence of the Nusselt number has been measured and comparison with the two theories [4, 25] became possible. The first experiments were done with water and helium RB cells. However, comparing  $Nu$  in water and in helium convection only allows for a small variation of the Prandtl number. From such experiments a small decrease of  $Nu$  with increasing  $Pr$  at given  $Ra$  was reported [27]: For  $Ra = 10^9$  Belmonte et al. [27] measured  $Nu = 76 \pm 11$  for  $Pr = 0.7$  and  $Nu = 48 \pm 6$  for  $Pr = 6.6$ . Much larger  $Pr$  variations are possible if RB convection in mercury or liquid sodium is studied. Those experiments with a mercury RB cell ( $Pr = 0.025$ ) by Rossby [28], by Takeshita et al. [15], and by Cioni et al. [11, 17] and with a liquid sodium RB cell ( $Pr = 0.005$ ) by Horanyi et al. [29] reveal that  $Nu$  *increases* with  $Pr$ , which is consistent with the Cioni et al. [17] extension of the Chicago mixing zone model.

However, there seems to be indication that also the Chicago mixing zone model cannot account for all phenomena observed in recent experiments: One of the most startling observations is that there seems to be a small but significant trend of the scaling exponent  $\gamma$  as a function of  $Pr$ . For  $Pr \approx 5 - 7$  (water) one has  $\gamma = 0.28 - 0.293$  [10, 22, 30, 31] for  $Ra$  up to  $Ra \approx 10^9$  and an even larger  $\gamma \approx 1/3$  for larger  $Ra \approx 10^9 - 10^{11}$  [32]; for  $Pr = 0.7 - 1$  (helium gas) it is  $\gamma = 0.282 \pm 0.006$  [4]; for  $Pr = 0.025$  (mercury)  $\gamma = 0.247$  [28] and  $\gamma = 0.26 \pm 0.02$  [17] (for  $Ra < 10^9$ ) have been measured; and for  $Pr = 0.005$  (liquid sodium) it is  $\gamma = 0.25$  [29]. Those and further experimental results are summarized in table I. All exponents between 0.25 and 0.33 have been measured! For thermal convection in a water RB cell ( $Pr \approx 5 - 7$ ) with self similarly distributed balls on the top and bottom wall, the scaling exponent can even be as large as  $\gamma = 0.45$ , presumably depending on the ball size distribution [33].

Next, a *breakdown* of the  $\gamma \approx 2/7$  scaling regime at very large  $Ra$  has recently been observed, possibly towards a scaling regime  $Nu \sim Ra^{1/2}$ , which has been predicted by Kraichnan decades ago [37]. For  $Pr = 0.025$  Cioni et al. [17] see the breakdown at  $Ra \sim 2 \cdot 10^9$  (and a startling small window with a local scaling exponent *smaller* than  $2/7$  for  $Ra \sim 5 \cdot 10^8 - 2 \cdot 10^9$ ) while for  $Pr = 0.7 - 1.0$  Chavanne et al. [19] observe it at  $Ra \sim 10^{11}$ . The transition around  $Ra \approx 10^{11}$  in figure 3 of ref. [10], showing  $Nu/Ra^{2/7}$  vs  $Ra$  from Wu and Libchaber's data [6, 38], may already be interpreted as the same breakdown. On the other hand, Glazier et al. [36] do not observe such a transition. Thus, the experimental situation itself is not yet clear.

All these observations and also the more intuitive rather than equation of motion based approach of ref. [4] call for a re-examination and extension of the existing scaling theories for thermal convection. Of course, a mathematically rigorous derivation of  $Nu(Ra, Pr)$  and  $Re(Ra, Pr)$  is hardly possible. The known rigorous bounds overestimate the measured Nusselt numbers by more than one order of magnitude and are only able to give the scaling exponent of the Kraichnan regime  $\gamma = 1/2$  [39–41].

Though in shortage of a strict mathematical derivation, the guideline of the presented approach will be the dynamical equations for the velocity field  $\mathbf{u}(\mathbf{x}, t)$ , the kinematic pressure

Reference	fluid	$Pr$	$Ra$ range	$\gamma$
Ashkenazi & Steinberg [34]	SF <sub>6</sub>	1 – 93	$10^9 - 10^{14}$	$0.30 \pm 0.03$
Garon & Goldstein [30]	H <sub>2</sub> O	5.5	$10^7 - 3 \cdot 10^9$	0.293
Tanaka & Miyata [31]	H <sub>2</sub> O	6.8	$3 \cdot 10^7 - 4 \cdot 10^9$	0.290
Goldstein & Tokuda [32]	H <sub>2</sub> O	6.5	$10^9 - 2 \cdot 10^{11}$	1/3
Qiu & Xia [20]	H <sub>2</sub> O	$\approx 7$	$2 \cdot 10^8 - 2 \cdot 10^{10}$	0.28
Lui & Xia [22]	H <sub>2</sub> O	$\approx 7$	$2 \cdot 10^8 - 2 \cdot 10^{10}$	$0.28 \pm 0.06$
Shen et al. [14]	H <sub>2</sub> O	$\approx 7$	$8 \cdot 10^7 - 7 \cdot 10^9$	$0.281 \pm 0.015$
Threlfall [35]	He	0.8	$4 \cdot 10^5 - 2 \cdot 10^9$	0.280
Castaing et al. [4]	He	0.7 – 1	$\lesssim 10^{11}$	$0.282 \pm 0.006$
Wu & Libchaber [6]	He	0.6 – 1.2	$4 \cdot 10^7 - 10^{12}$	0.285
Chavanne et al. [19]	He	0.6 – 0.73	$3 \cdot 10^7 - 10^{11}$	2/7
Davis [1]	air	$\approx 1$	$\lesssim 10^8$	0.25
Rosby [28]	Hg	0.025	$2 \cdot 10^4 - 5 \cdot 10^5$	0.247
Takeshita et al. [15]	Hg	0.025	$10^6 - 10^8$	0.27
Cioni et al. [17]	Hg	0.025	$5 \cdot 10^6 - 5 \cdot 10^8$	$0.26 \pm 0.02$
Cioni et al. [17]	Hg	0.025	$4 \cdot 10^8 - 2 \cdot 10^9$	0.20
Glazier et al. [36]	Hg	0.025	$2 \cdot 10^5 - 8 \cdot 10^{10}$	$0.29 \pm 0.01$
Horanyi et al. [29]	Na	0.005	$\lesssim 10^6$	0.25

TABLE I. Power law exponents  $\gamma$  of the power law  $Nu \sim Ra^\gamma$  for various experiments. The experiments were done with different aspect ratios, however, no strong dependence of the scaling exponent  $\gamma$  on the aspect ratio is expected (in contrast to the prefactors).

field  $p(\mathbf{x}, t)$ , and the temperature field  $\theta(\mathbf{x}, t)$ ,

$$\partial_t u_i + u_j \partial_j u_i = -\partial_i p + \nu \partial_j^2 u_i + \beta g \delta_{i3} \theta, \quad (5)$$

$$\partial_t \theta + u_j \partial_j \theta = \kappa \partial_j^2 \theta, \quad (6)$$

assisted by the appropriate boundary conditions at the bottom wall  $z = 0$ , the top wall  $z = L$ , and the side walls of the cell. Here,  $g$  is the gravitational acceleration,  $\beta$  the isobaric thermal expansion coefficient,  $\nu$  the kinematic viscosity,  $\kappa$  the thermal diffusivity, and  $L$  the height of the RB cell; the temperature difference between top and bottom walls is called  $\Delta$ .

The second feature of our approach introduced in section II is that we try to be as systematic as possible. We will be able to identify four different main scaling regimes for  $Re$  and  $Nu$  in the  $Ra - Pr$  phase space, depending on whether the BL or the bulk dominates the *global* thermal and kinetic energy dissipation, respectively. Three of the four regimes consist of two subregimes, depending on whether the thermal BL or the viscous BL is thicker. We also calculate the validity range the scaling laws and make predictions on the stability of the different regimes. In section III we compare the power law exponents of the theory with experimental data. In section IV we try to adopt the prefactors of the theory to some experimental information and compare the resulting prefactors to further experiments. Section V contains a summary and conclusions.

## II. BOUNDARY LAYER VS BULK DOMINANCE OF KINETIC AND THERMAL DISSIPATION

### A. Definitions

The parameter space of RB convection is spanned by the Rayleigh and by the Prandtl numbers,

$$Ra = \frac{\beta g L^3 \Delta}{\kappa \nu}, \quad Pr = \frac{\nu}{\kappa}. \quad (7)$$

Our main focus is on the resulting Reynolds and Nusselt numbers,

$$Re = \frac{UL}{\nu}, \quad Nu = \frac{\langle u_z \theta \rangle_A - \kappa \partial_3 \langle \theta \rangle_A}{\kappa \Delta L^{-1}}, \quad (8)$$

where  $\langle \cdot \rangle_A$  denotes the average over (any) z-plane. Correspondingly,  $\langle \cdot \rangle_V$  used below denotes the volume average.  $U$  is the mean large scale velocity near the boundaries of the cell. It is the remainder of the convection rolls which in the turbulent regime manifests itself as coherent large scale convection flow, as first discovered by Krishnamurti and Howard [42] and later found by various groups [4, 10, 20, 27, 38, 43–46]. The existence of this “wind of turbulence” is one of the central assumptions of our theory. We consider this to be a weak assumption, given the overwhelming experimental evidence. The effect of the wind is twofold: (i) In the range between the wind and the cell wall a shear flow boundary layer will build up. (ii) The wind stirs the fluid in the bulk. In the presented theory we consider the velocity *fluctuations* in the bulk of the cell only as a *consequence* of the stirring by the large scale roll. Therefore, the Reynolds number  $Re$  based on the roll velocity rather than the one based on the fluctuations  $Re_{fluct}$  in the bulk is taken as the more appropriate one to theoretically describe the bulk turbulence.

### B. Decomposition of the energy dissipation

The starting points of the present theory are the kinetic and thermal dissipation rates

$$\epsilon_u(\mathbf{x}, t) = \nu (\partial_i u_j(\mathbf{x}, t))^2, \quad (9)$$

$$\epsilon_\theta(\mathbf{x}, t) = \kappa (\partial_i \theta(\mathbf{x}, t))^2. \quad (10)$$

Their *global averages*  $\langle \epsilon_u(\mathbf{x}, t) \rangle_V = \epsilon_u$  and  $\langle \epsilon_\theta(\mathbf{x}, t) \rangle_V = \epsilon_\theta$  obey the following *rigorous* relations, which are easily derivable from the equations of motion, see e.g. [10, 25]:

$$\epsilon_u = \frac{\nu^3}{L^4} (Nu - 1) Ra Pr^{-2}, \quad (11)$$

$$\epsilon_\theta = \kappa \frac{\Delta^2}{L^2} Nu. \quad (12)$$

Dissipation takes place both in the bulk of the flow and in the boundary layers. Near the walls thermal and kinetic boundary layers of thicknesses  $\lambda_\theta$  and  $\lambda_u$  develop, which are determined

by the thermal diffusivity  $\kappa$  and the kinematic viscosity  $\nu$ , respectively, and which are in general different, depending on  $Pr$ . They are defined on the basis of the temperature and of the velocity profiles, respectively. Whenever there exists a thermal shortcut in the bulk due to the turbulent convective transport, the width of the thermal boundary layer is connected with the Nusselt number by

$$\lambda_\theta = \frac{1}{2} L Nu^{-1}. \quad (13)$$

The thickness of the kinetic boundary layer can be expressed in terms of the Reynolds number,

$$\lambda_u \sim L Re^{-1/2}. \quad (14)$$

Here, we have assumed that there is *laminar* viscous flow of Blasius type (cf. sects. 39 and 41 of ref. [47]) in the boundary layer; the lateral extension  $x$  of the BL has been identified with the height  $L$  of the cell, reflecting that the wind organizes in the form of a large scale roll. The transition to turbulence in the boundary layers will be considered in subsection II-F. Though for large enough  $Ra$  the total volume of the BLs is rather small, their contribution to the global average dissipation may be considerable, as the velocity and the temperature gradients in the BLs are much larger than in the bulk.

In general, we decompose the globally averaged dissipation rates into their BL and bulk contributions,

$$\epsilon_u = \epsilon_{u,BL} + \epsilon_{u,bulk}, \quad (15)$$

$$\epsilon_\theta = \epsilon_{\theta,BL} + \epsilon_{\theta,bulk}, \quad (16)$$

where  $\epsilon_{u,BL} = \int_{0 \leq z \leq \lambda_u} + \int_{L-\lambda_u \leq z \leq L} dz \nu (\partial_i u_j)^2 / L = \nu \langle (\partial_i u_j(\mathbf{x} \in BL, t))^2 \rangle_V$  is the viscous dissipation taking place in the viscous BL,  $\epsilon_{\theta,BL} = \int_{0 \leq z \leq \lambda_\theta} + \int_{L-\lambda_\theta \leq z \leq L} dz \kappa (\partial_i \theta)^2 / L = \kappa \langle (\partial_i \theta(\mathbf{x} \in BL, t))^2 \rangle_V$  is the thermal dissipation taking place in the thermal BL,  $\epsilon_{u,bulk} = \int_{\lambda_u \leq z \leq L-\lambda_u} dz \nu (\partial_i u_j)^2 / L = \nu \langle (\partial_i u_j(\mathbf{x} \in bulk, t))^2 \rangle_V$  is the viscous dissipation taking place in the bulk, etc.

This kind of thinking immediately suggests the existence of four regimes:

- (I) Both  $\epsilon_u$  and  $\epsilon_\theta$  are dominated by their BL contributions;
- (II)  $\epsilon_\theta$  is dominated by  $\epsilon_{\theta,BL}$  and  $\epsilon_u$  is dominated by  $\epsilon_{u,bulk}$ ;
- (III)  $\epsilon_u$  is dominated by  $\epsilon_{u,BL}$  and  $\epsilon_\theta$  is dominated by  $\epsilon_{\theta,bulk}$ ;
- (IV) both  $\epsilon_u$  and  $\epsilon_\theta$  are bulk dominated.

For (relatively) small  $Ra$  the BLs are most extended, therefore regime I is expected. On the other hand, for large  $Ra$  the BLs are very thin and we will expect regime IV, provided that the volume reduction of the BL is more efficient than the dissipation increase in the BLs due to the growing shear rate. Next, for small  $Pr$  the viscous BL is smaller than the thermal one,  $\lambda_u \ll \lambda_\theta$ , and we expect regime II. Finally, for large  $Pr$  it is  $\lambda_u \gg \lambda_\theta$  and we have regime III.

A priori it is not clear whether all four regimes can exist. However, after input of some experimental information, we will see that they are likely to exist. We will also calculate the scaling of the border lines between the different regimes in the  $Ra - Pr$  phase space. Of course, these lines do not indicate sharp transitions but the range of the change of dominance.

### C. Estimate of bulk and BL contributions

The next step is to estimate the various contributions  $\epsilon_{u,BL}$ ,  $\epsilon_{\theta,BL}$ ,  $\epsilon_{u,bulk}$ ,  $\epsilon_{\theta,bulk}$  of the BL and the bulk dissipation from the dynamical equations (5) and (6), expressing them as functions of  $Nu$ ,  $Re$ ,  $Ra$ , and  $Pr$ .

#### Bulk contributions:

We start with the *kinetic dissipation*. As already outlined above, the theory assumes that the bulk fluctuations with typical velocity  $u_{fluct}$  originate from the large scale coherent flow with velocity  $U$ . If there is no such “wind of turbulence”, the following estimates cease to be valid; the Reynolds number  $Re = UL/\nu$  even cannot be defined properly. Clearly, this will happen in the regime of very large Prandtl numbers where the flow is suppressed by the strong viscosity. Therefore, there will be a transition line  $Pr(Ra)$  in phase space, defined by, say,  $Re = 50$ , beyond which the theory no longer holds; we will calculate this line in section II-E. Another limit of applicability is in the very small  $Pr$  range. Here,  $\kappa$  is so large that the heat is molecularly conducted, thus  $Nu = 1$ . Other possible limitations of the basic assumptions of the theory will be discussed in section V.

The assumption of the large scale velocity  $U$  stirring the bulk implies the picture of a turbulent energy cascade in the bulk which in turn suggests how to estimate the *bulk* dissipation rates, namely by balancing the dissipation with the large scale convective term in the energy equations following from (5) and (6),

$$\epsilon_{u,bulk} = \nu \left\langle (\partial_i u_j(\mathbf{x} \in bulk, t))^2 \right\rangle_V \sim \frac{U^3}{L} = \frac{\nu^3}{L^4} Re^3 \quad (17)$$

As argued before, we took as the relevant velocity scale the wind velocity  $U$  and not the velocity fluctuations  $u_{fluct}$  because it is  $U$  which stirs the fluid in the bulk. This is a key assumption of the theory, justified by intuition and by the results. The presented theory does not make any statement on the  $Ra$ -scaling of the typical bulk fluctuations  $u_{fluct}$ .

We explicitly remark that the findings on the  $Re$  dependence of the energy dissipation rate in Taylor-Couette flow by Lathrop et al. [48] do *not* contradict eq. (17). Lathrop et al. [48] found that  $\epsilon_u L^4 \nu^{-3} Re^{-3}$  still depends on  $Re$  even for large  $Re$ . However, their result refers to the global  $\epsilon_u$ , *not* to  $\epsilon_{u,bulk}$ . – Possible intermittency corrections are not taken into consideration in eq. (17) as they are at most small [49].

We note that strictly speaking there should be a factor  $(L - 2\lambda_u)/L$  on the rhs of eq. (17), as the average  $\epsilon_{u,bulk} = \langle \epsilon_u(\mathbf{x} \in bulk, t) \rangle_V$  refers to the *whole* volume. However, it is assumed that the state is already turbulent enough, i.e.,  $Ra$  large enough, so that  $\lambda_u \ll L$ . The validity of this assumption limits the scaling ranges to be derived.

The estimate of the *thermal* bulk dissipation  $\epsilon_{\theta,bulk}$  is slightly more complicated, as the velocity field  $\mathbf{u}(\mathbf{x}, t)$  matters in the dynamical eq. (6) for the temperature. In particular, it matters whether the kinetic BL, characterized by a linear velocity profile, is nested in the thermal one or if it is the other way round.

For the former case ( $\lambda_u < \lambda_\theta$ , i.e., small  $Pr$ , the thermal boundary layer can be estimated in complete analogy to eq. (17) as

$$\epsilon_{\theta,bulk} = \kappa \left\langle (\partial_i \theta(\mathbf{x} \in bulk, t))^2 \right\rangle_V \sim \frac{U \Delta^2}{L} = \kappa \frac{\Delta^2}{L^2} Pr Re. \quad (18)$$

Note that in correspondence with  $U$  in eq. (17) we took the large scale temperature difference  $\Delta$  in eq. (18), not the typical temperature fluctuations  $\Delta_{fluct}$ . Again, this is a key assumption, justified by the later results.

For the latter case ( $\lambda_u > \lambda_\theta$ , i.e., large  $Pr$ , we must realize that at the merging of the (linear) thermal BL into the thermal bulk the velocity is *not*  $U$  itself, but smaller by a factor  $\lambda_\theta/\lambda_u < 1$ . Therefore, it is reasonable to assume that  $U\lambda_\theta/\lambda_u$  is the relevant velocity for the estimate of  $\epsilon_{\theta,bulk}$ , i.e.,

$$\epsilon_{\theta,bulk} \sim \frac{\lambda_\theta U \Delta^2}{\lambda_u L} = \kappa \frac{\Delta^2}{L^2} Pr Re^{3/2} Nu^{-1}. \quad (19)$$

BL contributions:

For  $\epsilon_{u,BL}$  we follow an idea by Chavanne et al. [19] and estimate, using eq. (14),

$$\epsilon_{u,BL} = \nu \left\langle (\partial_i u_j(\mathbf{x} \in BL, t))^2 \right\rangle_V \sim \nu \frac{U^2}{\lambda_u^2} \cdot \frac{\lambda_u}{L} \sim \frac{\nu^3}{L^4} Re^{5/2}. \quad (20)$$

Here,  $U/\lambda_u$  characterizes the order of magnitude of  $\partial_i u_j$  and the factor  $\lambda_u/L$  accounts for the BL fraction of the total volume. Again, this reasoning breaks down when there is no large scale “wind of turbulence”. Correspondingly, we estimate

$$\epsilon_{\theta,BL} = \kappa \left\langle (\partial_i \theta(\mathbf{x} \in BL, t))^2 \right\rangle_V \sim \kappa \frac{\Delta^2}{\lambda_\theta^2} \cdot \frac{\lambda_\theta}{L} \sim \kappa \frac{\Delta^2}{L^2} Nu. \quad (21)$$

Eqs. (17) to (21) express the various dissipation contributions (and thus the total dissipations  $\epsilon_u$  and  $\epsilon_\theta$ , (15) and (16)) in terms of  $Ra$ ,  $Pr$ ,  $Re$ , and  $Nu$ . If we insert eqs. (17) to (21) into the rigorous relations (11) and (12), we obtain two equations, allowing to express  $Nu$  and  $Re$  in terms of  $Ra$  and  $Pr$ . If we only take the dominating contributions  $\epsilon_{BL}$  or  $\epsilon_{bulk}$  in  $\epsilon_u$  and  $\epsilon_\theta$ , respectively, the formulae for the four regimes I, II, III, and IV are obtained, describing pure scaling instead of superpositions.

With this idea in mind, the scaling of the thermal boundary layer dissipation (21), though correct, does not give new information. It coincides with the rigorous relation (12). The physical reason is that the bulk is considered to provide a thermal shortcut. Therefore, we make use of the dynamics in the thermal BL in more detail. We approximate (systematically in order  $1/Re$ ) eq. (6) by the dominant terms (cf. [47] or [17, 25])

$$u_x \partial_x \theta + u_z \partial_z \theta = \kappa \partial_z^2 \theta \quad (22)$$

in the thermal BL. Both terms on the lhs are of the same order of magnitude as can be concluded from the incompressibility condition  $\partial_x u_x + \partial_z u_z \approx 0$ . In the lower subregimes with  $\lambda_u < \lambda_\theta$  the velocity  $u_x$  must be estimated by  $U$ , in the upper subregimes with  $\lambda_u > \lambda_\theta$  it is as argued above  $u_x \sim U\lambda_\theta/\lambda_u$ . In addition,  $\partial_x \sim 1/L$  and  $\kappa \partial_z^2 \sim \kappa/\lambda_\theta^2$ . Therefore, for  $\lambda_u < \lambda_\theta$  we finally get

$$Nu \sim Re^{1/2} Pr^{1/2} \quad (23)$$

and for  $\lambda_u > \lambda_\theta$  we have

$$Nu \sim Re^{1/2} Pr^{1/3}. \quad (24)$$

Eqs. (23) and (24) replace the correct (but useless) relation  $\epsilon_\theta \sim \epsilon_{\theta,BL}$  which does not add new information beyond (12).



## D. Four regimes

We will start with the  $\epsilon_{\theta,bulk}$  dominated regimes (III and IV).

Regime IV,  $\epsilon_u \sim \epsilon_{u,bulk}$  and  $\epsilon_\theta \sim \epsilon_{\theta,bulk}$  (large  $Ra$ )

Depending on whether  $\lambda_u$  is less or larger than  $\lambda_\theta$  we must use eq. (18) or eq. (19), respectively, for the  $\epsilon_{\theta,bulk}$ -estimate. The former happens for low  $Pr$ , the latter for large  $Pr$ . Therefore, we will give these two subregimes the index “l” for lower and “u” for upper. At what line  $Pr(Ra)$  in phase space  $\lambda_u = \lambda_\theta$ , the crossover from the  $\lambda_u < \lambda_\theta$  to the  $\lambda_u > \lambda_\theta$  will occur is not clear a priori. We will later calculate this line  $\lambda_u = \lambda_\theta$  with additional experimental information.

In regime  $IV_l$  we use (17) for  $\epsilon_u$  in (11) and (18) for  $\epsilon_\theta$  in (12) to obtain

$$Nu \sim Ra^{1/2} Pr^{1/2}, \quad (25)$$

$$Re \sim Ra^{1/2} Pr^{-1/2}. \quad (26)$$

We recognize the asymptotic Kraichnan regime [37], just as expected for large  $Ra$  when both thermal and kinetic energy dissipation are bulk dominated. Note that other lines of arguments can also lead to eq. (25), see e.g. Kraichnan’s work itself [37], Spiegel [50], or our reasoning in section II-F. Therefore, eq. (25) seems to be quite robust. The physics of this regime is that the dimensional heat current  $Nu\kappa\Delta/L$  is independent of both  $\kappa$  and  $\nu$ .

In regime  $IV_u$  we substitute as before (17) for  $\epsilon_u$  into eq. (11) but now (19) instead of (18) for  $\epsilon_\theta$  into eq. (12) to obtain

$$Nu \sim Ra^{1/3}, \quad (27)$$

$$Re \sim Ra^{4/9} Pr^{-2/3}. \quad (28)$$

The  $Nu$  scaling is the one also following from the Malkus theory [2].

Regime III,  $\epsilon_u \sim \epsilon_{u,BL}$  and  $\epsilon_\theta \sim \epsilon_{\theta,bulk}$  (large  $Pr$ )

Again we have to distinguish between the lower subregime  $III_l$  with  $\lambda_u < \lambda_\theta$  and the upper one  $III_u$  with  $\lambda_u > \lambda_\theta$ . For  $III_l$  we combine (20) with (11) and (18) with (12) and get

$$Nu \sim Ra^{2/3} Pr^{1/3}, \quad (29)$$

$$Re \sim Ra^{2/3} Pr^{-2/3}. \quad (30)$$

This regime will turn out to be small and less important. The more important one is  $III_u$ : Combine (20) with (11) and (19) with (12) to obtain

$$Nu \sim Ra^{3/7} Pr^{-1/7}, \quad (31)$$

$$Re \sim Ra^{4/7} Pr^{-6/7}. \quad (32)$$

This regime may be observable for large enough  $Pr$  when  $\lambda_u \gg \lambda_\theta$ . To our knowledge up to date this regime has neither been observed nor predicted.

Later, we will find hints for this regime  $III_u$  in form of a subleading correction to describe the Chavanne et al. data [19]. It would be nice to perform further experiments with large  $Pr$  to be able to more cleanly identify this postulated regime  $III_u$ . We note that this regime is *not* in contradiction to Chan’s [51] upper estimate  $Nu \leq const Ra^{1/3}$ , holding in the infinite

$Pr$  limit (for fixed  $Ra$ ), and also not in contradiction to Constantin and Doering's [52] rigorous upper bound  $Nu \leq const Ra^{1/3} (1 + \log Ra)^{2/3}$ , holding in the same  $Pr \rightarrow \infty$  limit. The reason is that regime  $III_u$  is for finite  $Pr$ ; if  $Pr \rightarrow \infty$ , also  $Ra \rightarrow \infty$ , if one wants to stay in regime  $III_u$ .

Regime II,  $\epsilon_u \sim \epsilon_{u,bulk}$  and  $\epsilon_\theta \sim \epsilon_{\theta,BL}$  (small  $Pr$ )

Regime  $II_l$ : Combining (17) with (11) gives together with (23)

$$Nu \sim Ra^{1/5} Pr^{1/5}, \quad (33)$$

$$Re \sim Ra^{2/5} Pr^{-3/5}. \quad (34)$$

This regime should show up for small enough  $Pr$  when  $\lambda_u \ll \lambda_\theta$ . Indeed, Cioni et al. [17] observed experimental hints for such a regime; also eqs. (33) – (34) have already been derived by them in a similar way [17]. A power law  $Nu \sim Ra^{1/5}$  was already suggested by Roberts [53].

Regime  $II_u$ : Because of the two competing conditions  $\epsilon_\theta \sim \epsilon_{\theta,BL}$  (i.e.,  $Pr$  small) and  $\lambda_u > \lambda_\theta$  (i.e.,  $Pr$  large) such a subregime can at most be small. It will turn out later that it will probably not exist altogether. Nevertheless, for completeness we give the scaling laws, resulting from taking now (24) and, as before, inserting (17) into (11), namely

$$Nu \sim Ra^{1/5}, \quad (35)$$

$$Re \sim Ra^{2/5} Pr^{-2/3}. \quad (36)$$

regime	dominance of	BLs	$Nu$	$Re$
$I_l$	$\epsilon_{u,BL}, \epsilon_{\theta,BL}$	$\lambda_u < \lambda_\theta$	$0.27 Ra^{1/4} Pr^{1/8}$	$0.037 Ra^{1/2} Pr^{-3/4}$
$I_u$		$\lambda_u > \lambda_\theta$	$0.33 Ra^{1/4} Pr^{-1/12}$	$0.039 Ra^{1/2} Pr^{-5/6}$
$II_l$ ( $II_u$ )	$\epsilon_{u,bulk}, \epsilon_{\theta,BL}$	$\lambda_u < \lambda_\theta$ $\lambda_u > \lambda_\theta$	$0.97 Ra^{1/5} Pr^{1/5}$ ( $\sim Ra^{1/5}$ )	$0.47 Ra^{2/5} Pr^{-3/5}$ ( $\sim Ra^{2/5} Pr^{-2/3}$ )
$III_l$ $III_u$	$\epsilon_{u,BL}, \epsilon_{\theta,bulk}$	$\lambda_u < \lambda_\theta$ $\lambda_u > \lambda_\theta$	$6.43 \cdot 10^{-6} Ra^{2/3} Pr^{1/3}$ $3.43 \cdot 10^{-3} Ra^{3/7} Pr^{-1/7}$	$5.24 \cdot 10^{-4} Ra^{2/3} Pr^{-2/3}$ $6.46 \cdot 10^{-3} Ra^{4/7} Pr^{-6/7}$
$IV_l$ $IV_u$	$\epsilon_{u,bulk}, \epsilon_{\theta,bulk}$	$\lambda_u < \lambda_\theta$ $\lambda_u > \lambda_\theta$	$4.43 \cdot 10^{-4} Ra^{1/2} Pr^{1/2}$ $0.038 Ra^{1/3}$	$0.036 Ra^{1/2} Pr^{-1/2}$ $0.16 Ra^{4/9} Pr^{-2/3}$

TABLE II. The power laws for  $Nu$  and  $Re$  of the presented theory, including the prefactors which are adopted to four pieces of experimental information in section IV. The exact values of the prefactors depend also on how the Reynolds number is defined, see the first paragraph of section IV. Regime  $II_u$  is put into brackets as it turns out that it does not exist for this choice of prefactors.

Regime I,  $\epsilon_u \sim \epsilon_{u,BL}$  and  $\epsilon_\theta \sim \epsilon_{\theta,BL}$

Regime  $I_l$ : This is the regime of (comparatively) small  $Ra$  whose scaling we obtain from using (23) and substituting (20) for  $\epsilon_u$  in (11), namely

$$Nu \sim Ra^{1/4} Pr^{1/8}, \quad (37)$$

$$Re \sim Ra^{1/2} Pr^{-3/4}. \quad (38)$$

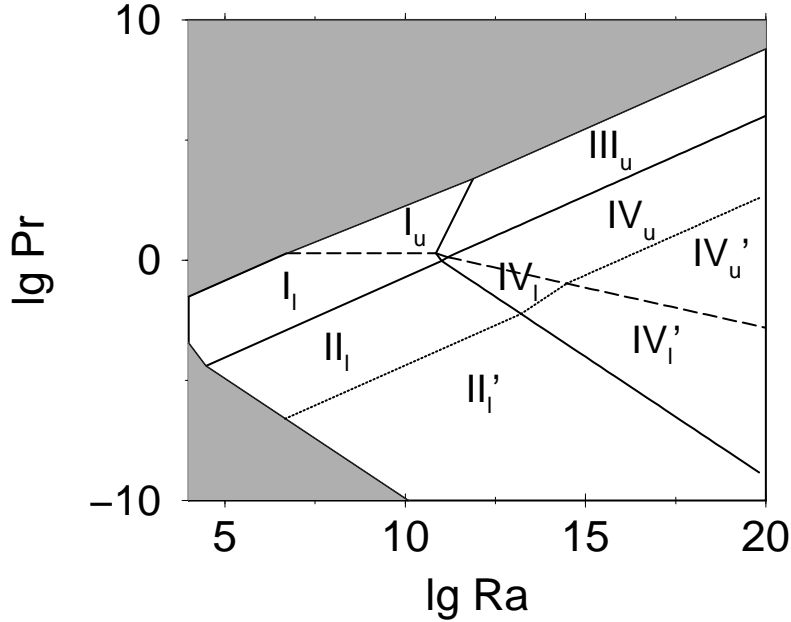


FIG. 1. Phase diagram in the  $Ra - Pr$  plane. The power laws and the corresponding prefactors (to be determined in section IV) in the respective regimes are summarized in table II. The tiny regime right of regime  $I_l$  is regime  $III_l$ . On the dashed line it is  $\lambda_u = \lambda_\theta$ . In the shaded regime for large  $Pr$  it is  $Re \leq 50$ , in the shaded regime for low  $Pr$  we have  $Nu = 1$ . The dotted line indicates the nonnormal-nonlinear onset of turbulence in the BL shear flow discussed in subsection II-F. The scaling in regime  $II'_l$  is therefore as in the bulk dominated regime  $IV_l$ . – The power laws for the boundaries between the different regimes are given in table III.

We argue that this is the regime whose scaling behavior has been observed in almost all thermal turbulence experiments [3–7, 9–11, 15–20, 22, 46], but that in nearly all cases the pure scaling behavior (37) and (38) has been polluted by sub-dominant contributions from the neighboring regimes, as we will elaborate in detail in the next section.

Remarkably, it is this power law  $Nu \sim Ra^{1/4}$  which was the first one suggested [1] and which has been well known in the engineering literature for a long time [54]. It also holds for two-dimensional convection in the low Prandtl number limit [55, 56].

Regime  $I_u$ : The scaling in  $I_u$  is obtained from equation (24) and combining (20) with (11), namely

$$Nu \sim Ra^{1/4} Pr^{-1/12}, \quad (39)$$

$$Re \sim Ra^{1/2} Pr^{-5/6}. \quad (40)$$

Note that the  $Ra$  dependence is the same as in  $I_l$ , but now  $Nu$  decreases with increasing  $Pr$ . This behavior is physically to be expected because due to increasing  $\nu$  the convective heat

transport is more and more reduced. And indeed, such a crossover from increase to decrease of  $Nu$  with  $Pr$  has been observed in experiment. It will later give us the opportunity to determine the transition line  $\lambda_u = \lambda_\theta$ .

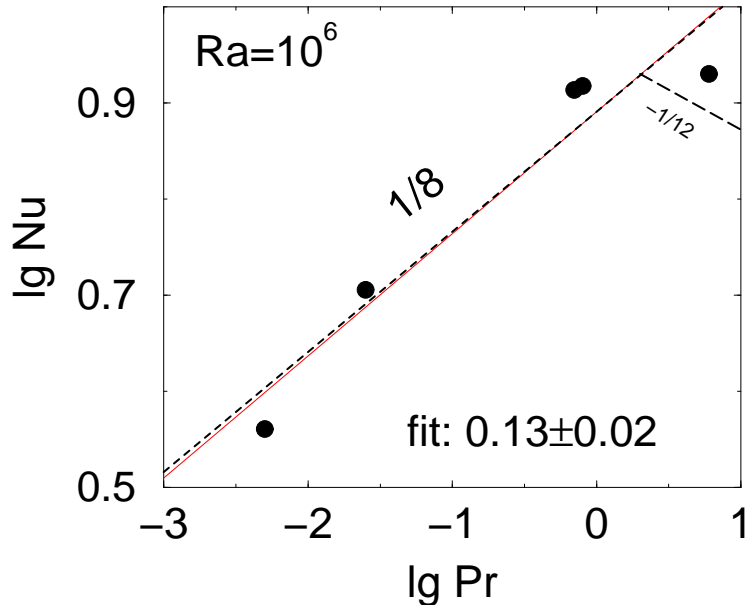


FIG. 2.  $Nu$  vs  $Pr$  for fixed  $Ra = 10^6$ . The fit is based on all points. The expected power law  $Nu \sim Pr^{1/8}$  in regime  $I_l$  is also shown (dashed). For larger  $Pr \geq 2$  one enters regime  $I_u$  where  $Nu \sim Pr^{-1/12}$  (dashed) is expected.

The scaling of this crossover line can already be determined here from equating  $\lambda_\theta \sim L/Nu$  and  $\lambda_u \sim L/\sqrt{Re}$  in the respective regimes. We obtain

$$Pr_\lambda^{I_l - I_u} \sim Ra^0, \quad (41)$$

$$Pr_\lambda^{II_l - II_u} \sim Ra^0, \quad (42)$$

$$Pr_\lambda^{III_l - III_u} \sim Ra^{-1/2}, \quad (43)$$

$$Pr_\lambda^{IV_l - IV_u} \sim Ra^{-1/3}. \quad (44)$$

Because the line  $\lambda_u = \lambda_\theta$  obeys  $Pr = const$  in regime  $I$  it either is above or below the common corner point of all four regimes. Therefore it can go either through regime  $III$  or through regime  $II$ , but not through both. Thus either regime  $II_u$  will exist or regime  $III_l$ , never both of them.

We now calculate the scaling of the boundaries between the other different domains in the  $Ra - Pr$  phase space. The boundary between  $I$  and  $II$  is obtained by equating  $\epsilon_{u,BL} \sim \epsilon_{u,bulk}$ , those between  $I$  and  $III$  by equating  $\epsilon_{\theta,BL} \sim \epsilon_{\theta,bulk}$ , etc. The results are

$$Pr_{trans}^{I_i-II_i} \sim Ra_{trans}^{2/3}, \quad (45)$$

$$Pr_{trans}^{I_i-III_i} \sim Ra_{trans}^{-2}, \quad (46)$$

$$Pr_{trans}^{III_i-IV_i} \sim Ra_{trans}^1, \quad (47)$$

$$Pr_{trans}^{II_i-IV_i} \sim Ra_{trans}^{-1}, \quad (48)$$

$$Pr_{trans}^{I_u-III_u} \sim Ra_{trans}^3, \quad (49)$$

$$Pr_{trans}^{III_u-IV_u} \sim Ra_{trans}^{2/3}. \quad (50)$$

Note that all these lines indicate the range of smooth crossover in the dominance of either the BL or the bulk dissipation.

The phase diagram in  $Ra - Pr$  phase space with the various regimes and crossovers is shown in figure 1, anticipating the prefactors of the power laws, whose exponents we have evaluated up to now. We will determine the prefactors in eqs. (23) – (50) in section IV from four pieces of experimental information. These experimental informations all come from experiments with an aspect ratio of the RB cell of the order of 1. We expect the prefactors to depend on the aspect ratio; therefore, all prefactors given in this paper only refer to aspect ratio order of 1 experiments.

### E. Range of validity of power laws

What is the range of validity of the power laws summarized in table II? For too small Reynolds numbers towards larger  $Pr$ , say,  $Re_{crit} = 50$ , the distinction between the bulk and the boundary layer is no longer meaningful; the bulk will no longer be driven to turbulence by a large scale velocity  $U$ . Correspondingly, if the Nusselt number approaches 1 because of too small  $Pr$ , the splitting of  $\epsilon_\theta$  in  $\epsilon_{\theta,BL}$  and  $\epsilon_{\theta,bulk}$  becomes meaningless. Finally, for  $Nu = 1$ , we no longer have thermal convection but pure thermal diffusion.

Therefore, we impose the restrictions  $Re \lesssim 50$  towards large  $Pr$  and  $Nu \gtrsim 1$  towards small  $Pr$ . The lines  $Re = 50$  and  $Nu = 1$  are included in above phase diagram figure 1. Their analytical forms directly follow from the power laws of table II; they are given in table III.

Beyond these lines, in the shaded areas in figure 1, the flow is viscosity dominated or thermal diffusivity dominated and the proposed power laws for  $Re$  and  $Nu$  (table II) no longer apply.

### F. Turbulence transition of the laminar boundary layer

For very large  $Ra$  the theory outlined here requires an extension. It is based so far on the existence of a laminar boundary layer flow of Blasius type; its thickness therefore obeys  $\lambda_u \sim LRe^{-1/2}$ , cf. section 39 of ref. [47]. The shear in this boundary layer is determined by the large scale velocity  $U$  of the thermal roles in the RB cell and the boundary layer width  $\lambda_u$ . We define the corresponding shear Reynolds number as

$$Re_{shear} = \frac{U\lambda_u}{\nu} \sim \sqrt{Re}. \quad (51)$$

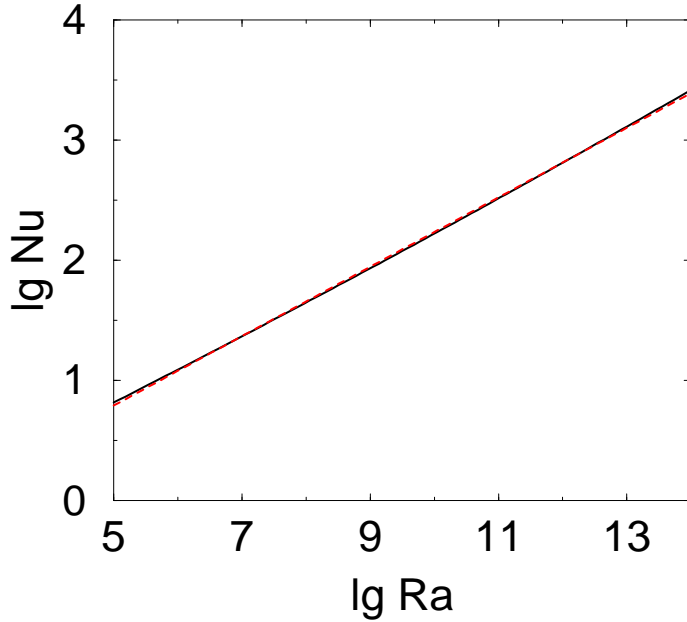


FIG. 3.  $Nu$  vs  $Ra$  for fixed  $Pr = 1$  (characterizing helium) according to the presented theory, i.e., equation (56) (solid line). Also shown is the practically indistinguishable result  $Nu = 0.22Ra^{0.289}$  of a linear regression of (56) (dashed line), which mimicks a power law with an exponent close to  $2/7$ .

The key issue now is that the laminar shear BL will become turbulent for large enough  $Re_{shear}$ . The details of the mechanism of this turbulence transition is still under study but it seems to have *nonnormal-nonlinear* [57–63] features. What however is agreed upon is that the shear Reynolds number at which the turbulence sets in depends on the kind and strength of the flow distortion. A typical value for the onset is [47]

$$Re_{shear,turb} = 420. \quad (52)$$

It will turn out that such high shear Reynolds numbers can only be achieved in regimes II and IV; in the regimes I and III the large Reynolds numbers necessary for the breakdown of the laminar shear BL are not achieved. With the information from table II we obtain the corresponding line in the  $Ra - Pr$  parameter space indicating the laminar-turbulence onset range, namely

$$Pr_{turb} \sim Ra_{turb}^{2/3} \quad (53)$$

in regimes  $II_l$  and  $IV_u$  (with different prefactors) and

$$Pr_{turb} \sim Ra_{turb}^1 \quad (54)$$

in regime  $IV_l$ . The corresponding prefactors will be calculated later, but for clarity we already included the characteristic lines which mark the onset to turbulence in the BL in the phase diagram figure 1 as dashed lines. Above, the Rayleigh-Benard rolls are still laminar in the boundary layer, below the boundary layer is turbulent.

What power laws for  $Re$  and  $Nu$  are to be expected in the regime beyond the turbulence transition of the laminar BL? One might argue that the destruction of the BL laminarity means that both the kinetic and the thermal dissipation rates scale as in the turbulent bulk. This implies that the scaling of  $Re$  and  $Nu$  should be the same as in the bulk dominated regime IV. In the phase diagram we called those regimes  $II'_l$ ,  $IV'_l$ , and  $IV'_u$ .

The same result is obtained by yet another argument: In a turbulent thermal boundary layer it holds [19, 47]

$$\frac{Lu_*}{\kappa} \sim Nu \log\left(\frac{Lu_*}{\kappa}\right). \quad (55)$$

With logarithmic precision the typical velocity scale  $u_*$  of the fluctuations in the BL is equal to the wind velocity  $U$  and therefore eq. (55) implies  $Nu \sim RePr$ . On the other hand, it still holds  $\epsilon_u \sim \epsilon_{u,bulk}$  or  $NuRaPr^{-2} \sim Re^3$ . From these two relations one immediately obtains the power laws (25) and (26), i.e., scaling as in regime  $IV_l$  for all three primed regimes  $II'_l$ ,  $IV'_l$ , and  $IV'_u$ .

Still we feel that further study is necessary to obtain reliable insight about the dissipation rate scaling in turbulent boundary layers. This might influence the scaling exponents in the primed regimes  $II'_l$  and  $IV'_{l,u}$ .

### III. COMPARISON WITH EXPERIMENT: SCALING EXPONENTS

#### A. Nusselt number

The first type of results of the theory which we would like to compare with experiments are the scaling exponents. First, we focus on the Nusselt number.

For fixed  $Ra = 10^6$  the  $Nu$  number seems to increase up to  $Pr \approx 7$ , see figure 2. The fit to the experimental data between  $Pr = 0.005$  and  $Pr \approx 7$  gives  $Nu \sim Pr^{0.13 \pm 0.02}$  in good agreement with the predicted exponent  $1/8$  in the regime  $I_l$ . We note, however, that the suggestion eq. (1) by Cioni et al. [17] is also consistent with experiment in the small  $Pr$  regime.

The increase with  $Pr$  seems to cease for  $Pr$  between 1 and 10. As stated above, other experimental data [27] even suggest a *decrease* of  $Nu$  with increasing  $Pr$  in that regime. This is compatible with and explained by the present theory which gives a ( $Ra$  number independent) transition from the  $I_l$  regime with  $Nu \sim Pr^{1/8}$  to  $I_u$  with  $Nu \sim Pr^{-1/12}$ , both for fixed  $Ra$ .

As there is even a controversy in literature whether  $Nu$  for water with  $Pr = 6.6$  or  $Nu$  for helium gas with  $Pr = 0.7$  is larger, it is hard to say where exactly the transition from  $I_l$  to  $I_u$  takes place. According to Cioni et al. [17] it is fair to say that within experimental accuracy  $Nu(Pr = 6.6) = Nu(Pr = 0.7)$ . We adopt this point of view and use it to calculate the transitional  $Pr$  number  $Pr_\lambda^{I_l - I_u}$  to be about 2. This experimental information thus defines

boundary between	$Pr_{trans}$
$I_l - II_l$	$Pr_{trans} = 4.3 \cdot 10^{-8} Ra_{trans}^{2/3}$
$I_l - III_l$	$Pr_{trans} = 1.0 \cdot 10^{22} Ra_{trans}^{-2}$
$II_l - IV_l$	$Pr_{trans} = 9.7 \cdot 10^{10} Ra_{trans}^{-1}$
$III_l - IV_l$	$Pr_{trans} = 9.1 \cdot 10^{-12} Ra_{trans}^1$
$I_u - III_u$	$Pr_{trans} = 5.7 \cdot 10^{-33} Ra_{trans}^3$
$III_u - IV_u$	$Pr_{trans} = 4.8 \cdot 10^{-8} Ra_{trans}^{2/3}$
$I_l - I_u$	$Pr_\lambda = 2.0 Ra_{trans}^0$
$III_l - III_u$	$Pr_\lambda = 5.3 \cdot 10^5 Ra_{trans}^{-1/2}$
$IV_l - IV_u$	$Pr_\lambda = 7.3 \cdot 10^3 Ra_{trans}^{-1/3}$
$I_l$ -(Re=50)	$Pr_{trans} = 6.7 \cdot 10^{-5} Ra_{trans}^{2/3}$
$I_u$ -(Re=50)	$Pr_{trans} = 3.0 \cdot 10^{-3} Ra_{trans}^{3/5}$
$I_l$ -(Nu=1)	$Pr_{trans} = 3.5 \cdot 10^4 Ra_{trans}^{-2}$
$II_l$ -(Nu=1)	$Pr_{trans} = 1.2 Ra_{trans}^{-1}$
$III_u$ -(Re=50)	$Pr_{trans} = 2.9 \cdot 10^{-5} Ra_{trans}^{2/3}$
$II_l$ -(BL-turbul.)	$Pr_{trans} = 9.3 \cdot 10^{-12} Ra_{trans}^{2/3}$
$IV_l$ -(BL-turbul.)	$Pr_{trans} = 3.4 \cdot 10^{-16} Ra_{trans}^1$
$IV_u$ -(BL-turbul.)	$Pr_{trans} = 2.3 \cdot 10^{-11} Ra_{trans}^{2/3}$

TABLE III. Boundaries between the various regimes I through IV, towards the limiting regimes where  $Nu = 1$  (small  $Pr$ ) and  $Re = 50$  (large  $Pr$ ), and the nonnormal-nonlinear onset of shear turbulence (last three lines, see section II-F).



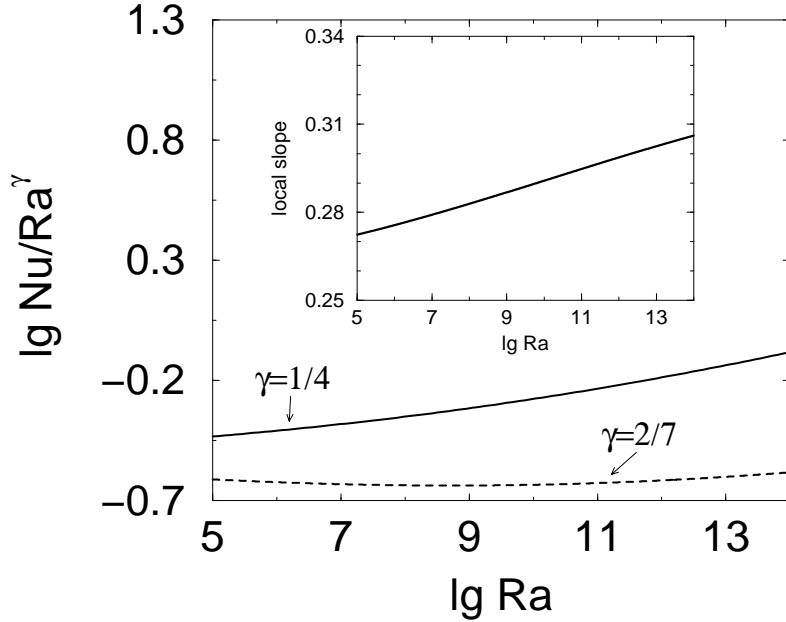


FIG. 4. The  $Nu$  number, as it follows from eq. (56, compensated by two different power laws  $Ra^{1/4}$  (solid, as suggest by the present theory for the low  $Ra$  regime) and  $Ra^{2/7}$  (dashed). The second is hardly distinguishable from a straight line, i.e., pure  $2/7$  scaling. The inset shows the local slope following from eq. (56).

the line  $\lambda_u = \lambda_\theta$  in the phase space and separates the lower subregime  $I_l$  with  $\lambda_u < \lambda_\theta$  from the upper subregime  $I_u$  with  $\lambda_u > \lambda_\theta$ .

Next, we compare the predicted scaling exponent  $\gamma$  of  $Nu$  vs  $Ra$ , which in regime I is according to the presented theory the same for the lower and the upper subregime. For small  $Pr$  (mercury, sodium) and (relatively) small  $Ra$  the theoretically obtained value  $\gamma = 1/4$  for the scaling exponent of  $Nu$  vs  $Ra$  has been measured in several experiments:  $\gamma = 0.247$  in [28],  $\gamma = 0.26 \pm 0.02$  in [17], and  $\gamma = 0.25$  in [29].

Also regime  $II_l$  (intermediate  $Ra$ , low  $Pr$ ) with  $\gamma = 1/5$  seems to have been observed by Cioni et al. [17].

For larger  $Pr$  (helium, water) the measured scaling exponent is larger,  $\gamma \approx 2/7$ , see table I. Here we argue that this results from the superposition of the scaling in regime I, with those in the regimes  $IV_u$  and  $III_u$ . To substantiate this, we plot the expected  $Nu$  vs  $Ra$  dependence for  $Pr = 1$ ,

$$Nu = 0.27Ra^{1/4} + 0.038Ra^{1/3}, \quad (56)$$

in figure 3. Here we have already made use of the prefactors from table II, which will be calculated in the next section. Now we fit eq. (56) with *one* power law in as large a regime

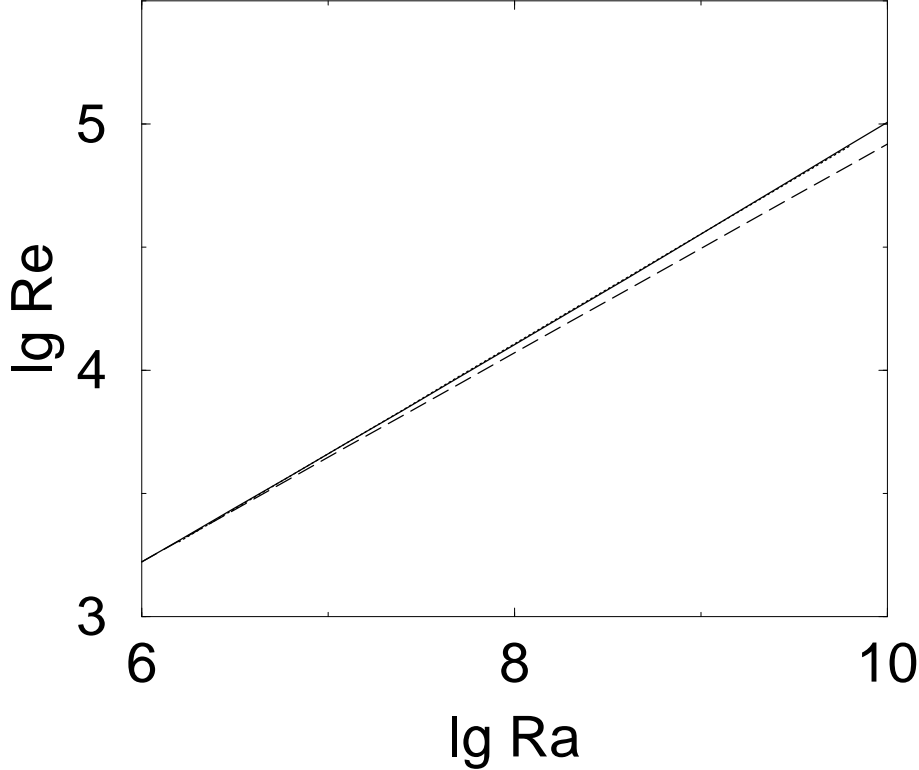


FIG. 5.  $Re$  vs  $Ra$  for mercury,  $Pr = 0.025$ . The solid line shows the theoretical superposition  $0.59Ra^{1/2} + 4.30Ra^{2/5}$  which is very well fitted by a straight line  $Re = 3.5Ra^{0.446}$  (dotted, practically indistinguishable from the solid line; the fit interval is  $Ra = 10^6$  to  $Ra = 4 \cdot 10^9$  as in experiment). The dashed line presents Cioni et al.'s fit through their data  $Re \propto Ra^{0.424}$ . The prefactors cannot be compared because of the different definitions of the Reynolds number in refs. [19] and [17], see section IV, first paragraph.

as  $10^5 \leq Ra \leq 10^{14}$ . This fit which is nearly indistinguishable from the superposition (56) reads

$$Nu = 0.22Ra^{0.289}. \quad (57)$$

The power law exponent is very close to  $2/7 = 0.286$  and definitely consistent with the experimental data of table I. Changing the fit regime of course changes the exponent of the power law (57). E.g., for a linear regression in the regime  $10^6 < Ra < 10^{11}$  which is typical for many experiments one obtains  $Nu = 0.24Ra^{0.285}$ , i.e., an exponent which is even closer to  $2/7$ .

By plotting compensated plots or local slopes  $d \log_{10} Nu / d \log_{10} Ra$  as done in figure 4 for eq. (56) one may be able to get hints that there is no pure power law. Note, that on first sight a compensation with  $Ra^{2/7}$  may erroneously even be considered as “better”.

Chavanne et al. [19] find hints for a transition to a regime with a visibly larger scaling exponent. According to our theory this could be regime  $III_u$  or  $IV_l$  or  $IV'_l$  or, most likely,

a mixture of all of them. No clean scaling exponent could hitherto be determined experimentally. One reason is that in that regime both  $Ra$  and  $Pr$  change. We will discuss the possible nature of this transition below. Also figure 3 of ref. [10] suggests such a transition.

We now turn to the large  $Pr$  regime. There are very few data for large  $Pr \gg 1$ . Recently, Ashkenazi and Steinberg [34] performed convection experiments with  $SF_6$  close to its critical point. In these experiments both  $Ra$  and  $Pr$  change considerably at the same time. To what degree the RB convection is still Boussinesq close to the critical point is extensively discussed in ref. [34].

Ashkenazi and Steinberg obtain  $Nu = 0.22Ra^{0.3 \pm 0.03}Pr^{-0.2 \pm 0.04}$  in  $10^9 \leq Ra < 10^{14}$  and  $1 \leq Pr \leq 93$ . Based on the phase diagram 1 we judge that for these ranges of the  $Ra$  and  $Pr$  numbers we should be in regimes  $I_u$  and  $III_u$ . From table II we see that the  $Ra$  exponent of  $Nu$  is  $1/4$  and  $3/7$ , respectively. The measured exponent of  $0.3 \pm 0.03$  in between is consistent with this. The  $Pr$  exponent of  $Nu$  is expected to be in between  $-1/12$  and  $-1/7$ , slightly smaller (modulus-wise) than the value of  $-0.2 \pm 0.04$  reported in [34].

The results of this subsection clearly demonstrate the importance of superimposing the power laws of adjacent phase space regimes. This can really mimic different scaling behavior, as demonstrated in figures 3 and 5. This characteristic feature holds because the power law exponents of the neighboring regimes are rather similar. They will commonly show up if data in a crossover range are examined. We emphasize that these crossover ranges appear to be rather extended, reaching well into the corresponding regimes, due to the small differences of the scaling exponents.

Therefore, rather than writing pure power laws, one should allow for superpositions. Table II suggests

$$Nu \sim Ra^{1/4}Pr^{1/8} \cdot \left( 1 + \begin{pmatrix} c_{III_u} Ra^{5/28} Pr^{-15/56} + \dots \\ c_{IV_u} Ra^{1/12} Pr^{-1/8} + \dots \\ c_{IV_l} Ra^{1/4} Pr^{3/8} + \dots \\ c_{II_l} Ra^{-1/20} Pr^{3/40} + \dots \end{pmatrix} \right) \quad (58)$$

and

$$Re \sim Ra^{1/2}Pr^{-3/4} \cdot \left( 1 + \begin{pmatrix} c'_{III_u} Ra^{1/14} Pr^{-3/28} + \dots \\ c'_{IV_u} Ra^{-1/18} Pr^{1/12} + \dots \\ c'_{IV_l} Pr^{1/4} + \dots \\ c'_{II_l} Ra^{-1/10} Pr^{3/20} + \dots \end{pmatrix} \right), \quad (59)$$

respectively. Here, we have separated the exponents of regime  $I_l$ . Which of these corrections and how many are to be taken depends on the  $Pr$  number and on the aspect ratio. *Locally*, i.e., for a limited  $Ra$  range, the suggested  $Nu$  vs  $Ra$  power law exponents  $\gamma = 2/7$  [4, 25] (cf. figure 2 of ref. [19] or figure 3 of [10]), or  $\gamma = 5/19$  [64] can still be considered as an appropriate representation of the experimental data. *Globally*, for larger  $Ra$  intervals, however, we claim that eq. (58) is a better description.

In previous publications  $Nu$ , compensated by the expected scaling  $Ra^{2/7}$ , was plotted against  $Ra$  in a log-log plot, see figure 2 of ref. [19]. From that plot one realizes that the  $2/7$ -scaling is slightly too steep between  $Ra = 10^6$  and  $Ra = 10^8$  and not steep enough beyond the crossover at  $Ra = 10^{11}$ . The analogously compensated plot with the expected scaling (37) is shown in figure 6. Now (for  $Pr \approx 1$ ) one obtains a horizontal line up to  $Ra \approx 10^9$ ,

showing that eq. (37) nicely agrees with the data. However, beyond  $Ra \approx 10^9$  one observes deviations. We suggest that these corrections originate from the different scaling in the neighboring regime  $III_u$ . The reason that it is regime  $III_u$  (and not regime  $IV_u$ ) is that in the Chavanne et al. experiments the large  $Ra$  measurements also have large  $Pr$ ; the trajectory in control parameter space  $Ra - Pr$  is not a straight line. At  $Ra = 10^{10}$  one typically has  $Pr \approx 1$ , but at  $Ra = 10^{14}$  Chavanne et al. typically have  $Pr \approx 10 - 20$ . The power law exponent  $5/28$ , following from table II, is consistent with the experimental data for large  $Ra$ , see figure 6.

For the mercury data of Cioni et al. [17] we do not have such a complication as  $Pr = 0.025$  is roughly constant for all chosen  $Ra$ . As plotted in figure 6, lower curve, we observe a straight line up to about  $2 \cdot 10^8$  and then a decay, signaling contributions from regime  $II_l$ . The power law exponent  $-1/20$  of the correction term in eq. (58) is consistent with the data shown in figure 6.

A more stringent way to test the superpositions of type (58) is to make a *linear* plot  $Nu/(Ra^{1/4}Pr^{1/8})$  vs  $Ra^{5/28}Pr^{-15/56}$  or vs  $Ra^{1/12}Pr^{-1/8}$  or vs  $Ra^{1/4}Pr^{3/8}$ , etc, depending on which neighboring regime the corrections originate. This is done in figure 7, assuming, as argued above, that the most relevant corrections originate from regime  $III_u$ . If the theory is correct, the data points must fall on a straight line. Indeed, they do so with satisfying precision.

Note that this kind of linear plot is very sensitive to what combinations of  $Ra$  and  $Pr$  are chosen as  $x$  and  $y$  axes. E.g., plotting  $Nu/(Ra^{1/4}Pr^{1/8})$  vs  $Ra^{1/4}Pr^{3/8}$  (the subleading correction characterizing regime  $IV_l$ ) does not lead to a straight line at all, see the inset of figure 7. Clearly the variable  $Ra^{5/28}Pr^{-15/56}$  on the abscissa is superior, adding confirmation that the Chavanne et al. [19] large  $Ra$  experiments represent the physics of regime  $III_u$ .

## B. Reynolds number

We now consider the experimental values for the scaling exponents  $\alpha$  of the Reynolds number vs the Rayleigh number. For  $Pr \approx 7$  (water) Xin et al. [46] find  $\alpha = 0.50 \pm 0.01$  and Qiu and Xia [20] find  $\alpha = 0.50 \pm 0.02$ . Both experiments were done in the  $Ra$  interval between  $2 \cdot 10^8$  and  $2 \cdot 10^{10}$ , i.e., in regime  $I_u$ , where exactly this power law exponent  $\alpha = 1/2$  is expected. For  $Pr \approx 1$  both Castaing et al. [4] and Chavanne et al. [19] find  $\alpha = 0.49$  for all  $Ra$  which suggests that possibly the regimes  $I_l$  and  $IV_l$  are seen where this value is predicted, or also regime  $III_u$ , where the exponent is only slightly higher ( $4/7$ ). For  $Pr = 0.025$  (mercury) Cioni et al. [17] find  $\alpha = 0.424$  from a fit to all available  $Ra$ . This value is in between the derived values  $\alpha = 1/2$  in regime  $I_l$  and  $\alpha = 2/5$  in regime  $II_l$ .

We compare this experimental finding  $Re \propto Ra^{0.424}$  (based on a fit to the data in the range up to  $Ra = 4 \cdot 10^9$  [17]) with the  $I_l$ - $II_l$  superposition according to table II

$$Re = 0.59Ra^{1/2} + 4.30Ra^{2/5}, \quad (60)$$

cf. fig. 5. In this relatively short  $Ra$  interval the theoretical superposition (60) is again hardly distinguishable from its straight line fit

$$Re = 3.5Ra^{0.446} \quad (61)$$

whose exponent reasonably well agrees with the measured one.<sup>2</sup>

Moreover, also the theoretically obtained  $Pr$  number dependence of  $Re$  very nicely agrees with available experimental information: Chavanne et al. [19] did experiments with (slightly) varying  $Pr$ . They then plotted  $RePr^{0.72}$  vs  $Ra$  and obtained the law  $RePr^{0.72} = 0.0374Ra^{1/2}$ . The exponent 0.72 of the Prandtl number was determined by minimizing the scattering of points around a straight line in the log-log plot. It very well agrees with the calculated  $Pr$  scaling exponent  $3/4$  in eq. (38) (regime  $I_l$ ). A possible reason for the slight difference between theory and data fit is that part of the experimentally realized  $Ra$  and  $Pr$  already belong to regimes  $III_u$  and  $IV_u$ , where according to eqs. (26) and (28) the expected  $Pr$  scaling exponent is  $6/7$  and  $2/3$ , respectively. However, the deviation is clearly within the experimental uncertainty. In figure 8 we replot the experimental Reynolds number data of Chavanne et al. [19]. In fig. 8a we show  $Re/Pr^{-3/4}$  vs  $Ra$ . The fit gives a  $Ra$ -exponent  $0.492 \pm 0.002$  in very good agreement with the theory's exponent  $1/2$ . In fig. 8b we display  $Re/Ra^{1/2}$  vs  $Pr$ . The data fit results in a  $Pr$ -exponent  $-0.77 \pm 0.01$ , also in excellent agreement with the theoretical expectation which is  $-3/4$  in  $I_l$  and  $-5/6$  in  $I_u$ .

The large  $Ra$  values in both figures will turn out to belong already to the regimes  $III_u$  and  $IV_u$ , where the  $Pr$ -scaling is similar. The available range is too small to perform a more detailed comparison.

The only large  $Pr$  data available are again those by Ashkenazi and Steinberg [34]. They obtain  $Re = 2.6Ra^{0.43 \pm 0.02}Pr^{-0.75 \pm 0.02}$  in  $10^{12} \leq Ra < 3 \cdot 10^{14}$  and  $27 \leq Pr \leq 190$ . The expected  $Ra$  exponent of  $Re$  is between  $1/2$  and  $4/7$ , distinctly larger than the measured one of  $0.43 \pm 0.02$ . Similarly, the theoretically expected  $Pr$  exponent of  $Re$  is between  $-5/6$  and  $-6/7$ , also larger than the measured exponent  $-0.75 \pm 0.02$ . We have no explanation.

## IV. PREFACTORS

### A. Experimental input to determine the prefactors

To obtain the values of the prefactors in the power laws within the presented scaling theory, we need further input from experiment. But what data to choose? As pointed out in the introduction, a huge variety of data is around, often disagreeing with each other even in the scaling exponents, not to speak of prefactors. Those often vary by as much as 50% from experiment to experiment, even for cells with the same aspect ratio. Another reason which makes the adoption to one experiment and the comparison to others difficult is that different definitions are used for the Reynolds numbers. E.g., Cioni et al. [17] define the Reynolds number as  $Re = 4L^2f_p/\nu$ , where  $f_p$  is a distinguished frequency at the small frequency edge in the temperature spectrum. Chavanne et al. [19] define  $Re = \omega_0 dL/\nu$ , where  $\omega_0$  is a

---

<sup>2</sup>The absolute values of the Reynolds numbers cannot be compared here, as the Reynolds number definitions in refs. [17] and [19] cannot be transferred into each other, see the first paragraph in section IV.

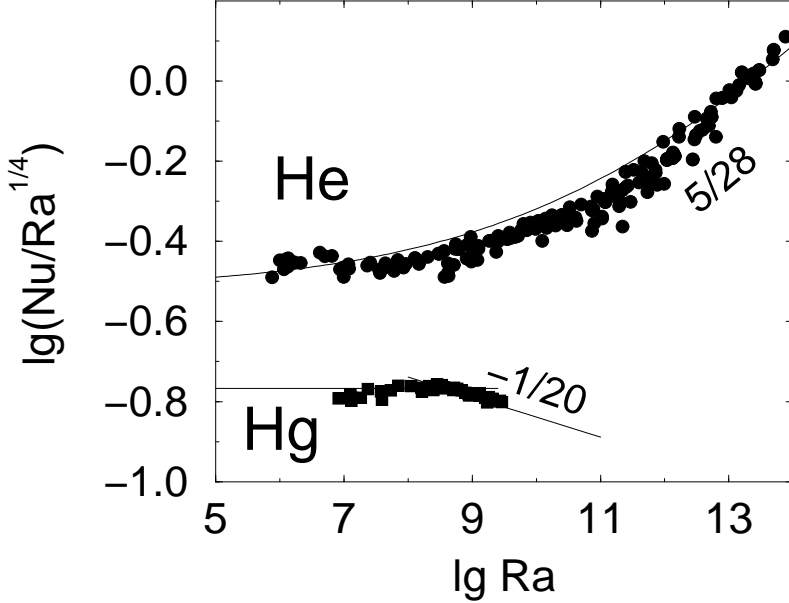


FIG. 6. Compensated  $Nu$  vs  $Ra$  data for  $Pr$  from about 1 through about 20 (helium, upper, data taken from ref. [19]; the higher  $Ra$  experiments also have higher  $Pr$ -number) and  $Pr = 0.025$  (mercury, lower, taken from ref. [17]). Also shown are the calculated exponents in the large  $Ra$  regimes. We also drew the theoretical curve  $Nu = 0.33Ra^{1/4}Pr^{-1/12} + 3.43 \cdot 10^{-3}Ra^{3/7}Pr^{-1/7}$  with fixed  $Pr = 3$  to demonstrate that it roughly describes the data. If the expected  $Pr$  number dependence is considered, the agreement becomes even better.

typical frequency in the cross correlation spectrum of two temperature signals, measured at a vertical distance of  $d = 2.3$  mm and 2 cm off the axis of the cell.

In spite of these difficulties, we decided to calculate the prefactors of the suggested scaling laws by employing the following choice for the input information as a reasonable, realistic example. Our reasons are first, to be able to draw a phase diagram with more or less realistic values. Second, to stress the importance of the prefactors. But we caution the reader that our input choice is somehow arbitrary; other possibilities can equally well be rationalized, sometimes shifting the various regime boundaries considerably.

Above, as an input from experiment, we had already chosen  $Pr_\lambda = 2$  as the Prandtl number for which  $Nu$  is maximal (for fixed  $Ra = 10^6$ , cf. fig. 2). In addition, we will use the following experimental information:

1. The observed transition Rayleigh number for the transition from regime  $I_l$  to regime  $III_l$ ,  $Ra_{trans} = 10^{11}$  at  $Pr = 1$  [19];

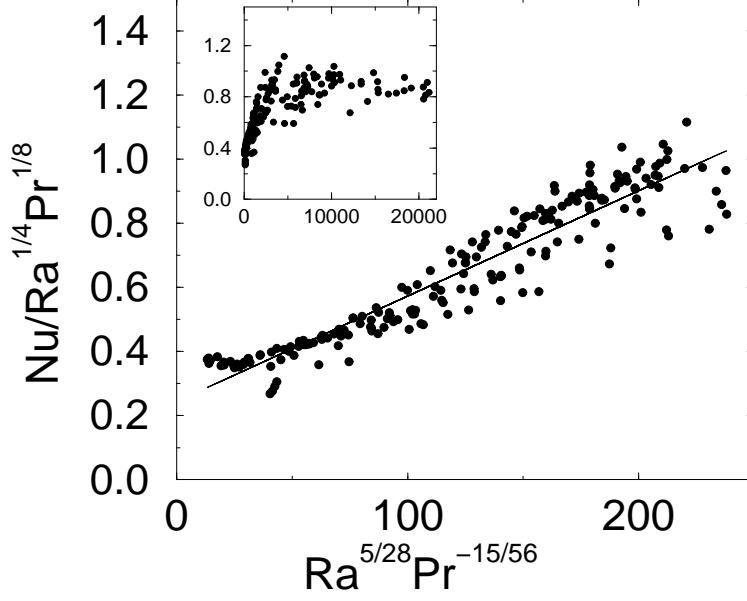


FIG. 7. Same data as in the previous figure, but now in a linear plot  $Nu/(Ra^{1/4}Pr^{1/8})$  vs  $Ra^{5/28}Pr^{-15/56}$ , revealing the quality of the superposition eq. (58), high  $Pr$ , regime  $III_u$ . The linear fit (straight line) gives  $Nu/(Ra^{1/4}Pr^{1/8}) = 0.24 + 3.3 \cdot 10^{-3} Ra^{5/28} Pr^{-15/56}$ . The data points are taken from ref. [19], with kind permission by the authors. Only data points with  $Ra > 10^6$  are considered. Note that in this plot  $Pr$  varies as much as  $0.6 < Pr < 100$ . – The inset shows  $Nu/(Ra^{1/4}Pr^{1/8})$  vs  $Ra^{1/4}Pr^{3/8}$ ; this variable had to be used if regime  $IV_l$  contributes the most relevant correction. The data do not fall on a straight line. A similar failure results with the regime  $IV_u$ -compensated variable  $Ra^{1/12}Pr^{-1/8}$ .

2. the observed transition Rayleigh number for the transition from regime  $I_l$  to regime  $II_l$ ,  $Ra_{trans} = 4.5 \cdot 10^8$  at  $Pr = 0.025$  [17];
3. the experimental values, taken from ref. [19], for the Reynolds and the Nusselt number at the middle point  $(Ra_M, Pr_M)$  in the phase diagram figure 1;
4. and the prefactor 0.0372 of the scaling law  $Re = 0.0372 Ra^{1/2} Pr^{-3/4}$  measured in regime  $I_l$  [19].

Information (1) specifies the prefactor of the rhs of eq. (46) (which we call  $c_{I_l-III_l}$ ) to be  $c_{I_l-III_l} = Pr_{trans}^{I_l-III_l} / Ra_{trans}^{-2} = 1.0 \cdot 10^{22}$ . Information (2) gives the prefactor of the rhs of eq. (45) (which we call  $c_{I_l-II_l}$ ) to be  $c_{I_l-II_l} = Pr_{trans}^{I_l-II_l} / Ra_{trans}^{2/3} = 4.3 \cdot 10^{-8}$ . The two curves (45) and (46) cross at

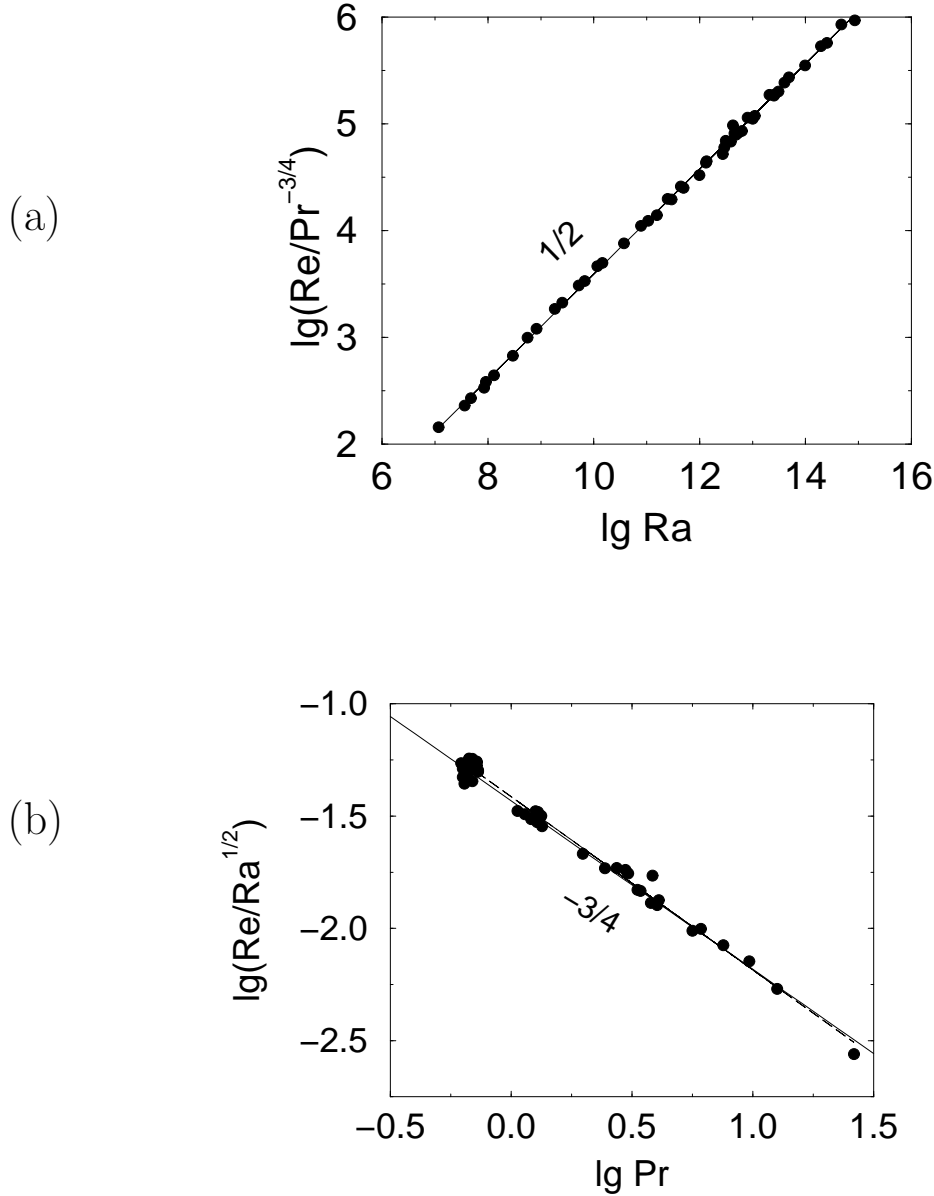


FIG. 8. The figure presents data for the Reynolds number as a function of  $Ra$  and  $Pr$  from ref. [19], with very kind permission of the authors.

a)  $Re/Pr^{-3/4}$  vs  $Ra$ . The expected slope is  $1/2$ , the linear regression fit (solid line) gives  $0.492 \pm 0.002$ .

b)  $Re/Ra^{1/2}$  vs  $Pr$ . The expected slope is  $-3/4$ , the linear regression fit (dashed line) gives  $-0.77 \pm 0.01$ . The agreement of the prefactor is also excellent. According to theory, following table II it is  $\log_{10}(Re/Ra^{1/2}) = -1.432 - (3/4)\log_{10} Pr$  (solid line, hardly distinguishable from the dashed one); the fit value for the prefactor from linear regression is  $-1.413 \pm 0.005$ .



$$(Ra_M, Pr_M) = (1.03 \cdot 10^{11}, 0.94). \quad (62)$$

This middle point  $(Ra_M, Pr_M)$  is defined by the conditions  $\epsilon_{u,BL} = \epsilon_{u,bulk} = \epsilon_u/2$  and  $\epsilon_{\theta,BL} = \epsilon_{\theta,bulk} = \epsilon_\theta/2$ . Equation (62) specifies the prefactors of the rhs of eqs. (47) and (48) to be  $c_{III_l-IV_l} = 9.1 \cdot 10^{-12}$  and  $c_{II_l-IV_l} = 9.7 \cdot 10^{10}$ , respectively. We see that  $Pr_\lambda^{I_l-I_u} = 2 > Pr_M = 0.94$  so that there is a regime  $III_l$ , but no regime  $II_u$ , as already anticipated. The line  $Pr_\lambda^{I_l-I_u} = 2$  hits the boundary between  $I$  and  $III$  at

$$(Ra_{M'}, Pr_{M'}) = (7.1 \cdot 10^{10}, 2.0), \quad (63)$$

which fixes the prefactors of eqs. (49) and (43) to be  $5.7 \cdot 10^{-33}$  and  $5.3 \cdot 10^5$ , respectively. Correspondingly, one obtains the prefactors of eqs. (50) and (44) to be  $4.8 \cdot 10^{-8}$  and  $7.3 \cdot 10^3$ , respectively. These are the data on which the phase diagram figure 1 is based; they are summarized in table III.

Apart from regime  $III_l$  all regimes turned out to have at least one decade of extension both in  $Ra$  and in  $Pr$  and should therefore in principle be visible. However, we should always expect one or more subleading corrections. Regime  $III_l$  will clearly not be detectable.

We again stress how dependent this phase diagram drawn in figure 1 is on the choice of experimental information. E.g., if we had adopted Glazier et al.'s [36] point of view that there is no transition towards a steeper  $Ra$  dependence of  $Nu$  at least up to  $Ra = 8 \cdot 10^{10}$ , regimes  $II$  and  $IV$  would have shifted further to the right or would even not exist at all. But as shown in figure 3, apparent smooth scaling behavior does *not* allow to exclude a transition.

Making use now of the experimental information (3) and (4) we can calculate the prefactors in the power laws for  $Nu$  and  $Re$ . From figs. 2 and 3 of Chavanne et al.'s work [19] we can extract the Reynolds and Nusselt numbers at the middle point  $(Ra_M, Pr_M)$  of the phase diagram which touches all four regimes, namely

$$Re_M = 1.20 \cdot 10^4, \quad Nu_M = 2.78 \cdot 10^2, \quad (64)$$

which is information (3) above. The definition of the middle point  $(Ra_M, Pr_M)$ , i.e., the conditions  $\epsilon_{u,BL} = \epsilon_{u,bulk} = \epsilon_u/2$  and  $\epsilon_{\theta,BL} = \epsilon_{\theta,bulk} = \epsilon_\theta/2$ , allows to calculate the prefactors  $c_{\epsilon_u,bulk}$ ,  $c_{\epsilon_\theta,bulk}$ , and  $c_{\epsilon_u,BL}$  on the rhs of eqs. (17), (18), and (20), respectively. One obtains

$$c_{\epsilon_u,bulk} = \frac{Nu_M Ra_M}{2Pr_M^2 Re_M^3} = 9.38, \quad (65)$$

$$c_{\epsilon_\theta,bulk} = \frac{Nu_M}{2Pr_M Re_M} = 0.0123, \quad (66)$$

$$c_{\epsilon_u,BL} = \frac{Nu_M Ra_M}{2Pr_M^2 Re_M^{5/2}} = 1028. \quad (67)$$

Finally, the prefactor  $c_{Nu}$  on the rhs of relation (23) is adopted to Chavanne et al.'s [19] experimentally determined prefactor (see figure 3 of that paper) in the relation (38), i.e.,  $Re = 0.0372 Ra^{1/2} Pr^{-3/4}$  valid throughout regime  $I_l$  (information (4) above). In that regime  $\epsilon_{u,BL} = \epsilon_u$ ; with eqs. (11), (20), and (67) we get

$$c_{Nu} = (3.72 \cdot 10^{-2})^2 \cdot c_{\epsilon_u, BL} = 1.42. \quad (68)$$

The prefactors referring to the upper halve of the phase diagram are calculated from the matching conditions for  $Re$  and  $Nu$  on the  $\lambda_u = \lambda_\theta$  line. With eqs. (65) – (68) and the matching conditions now *all* prefactors of the power laws in the four different regimes are determined. We have summarized all these power laws in table II.

Note that from the condition  $\lambda_u = \lambda_\theta$  for  $Pr = 2$  the prefactor of eq. (14) is also obtained. It is 0.25, i.e.,  $\lambda_u = 0.25LRe^{-1/2}$ . Also the prefactors to the  $Nu = 1$ - and the  $Re \leq 50$ -borders of validity and the crossover lines to turbulence of the laminar BL flow automatically follow, and are included into table II.

## B. Comparison of the evaluated prefactors to experiment

We now would like to compare the absolute agreement of the power laws summarized in table II, whose prefactors result from an adoption to above four pieces of experimental information, with *further* experimental data. We first focus on the Chavanne et al.'s [19] RB measurements in helium gas. From the previous section we know that in these experiments due to the large  $Pr$  at large  $Ra$  it is mainly regime  $III_u$  which causes additional contributions to regime  $I_l$ . Therefore, we have plotted the superposition  $Nu = 0.33Ra^{1/4}Pr^{-1/12} + 3.43 \cdot 10^{-3}Ra^{3/7}Pr^{-1/7}$  with  $Pr = 3$  into figure 6. We again stress that in the experiments  $Pr$  is not constant at all. Nevertheless, the data are satisfactorily described. Note that the solid curve in figure 6 is no fit!

A much better way to check whether the obtained prefactors of the theory agree with the measured ones is to do a linear regression of the straight line as offered in figure 7. Such a straight line fit gives  $Nu/(Ra^{1/4}Pr^{1/8}) = 0.24 + 3.3 \cdot 10^{-3}Ra^{5/28}Pr^{-15/56}$ . The found prefactors are in good agreement with the expectation  $Nu/(Ra^{1/4}Pr^{1/8}) = 0.27 + 3.43 \cdot 10^{-3}Ra^{5/28}Pr^{-15/56}$  from table II.

We also compare the theoretical prefactors of the Reynolds number scaling in regime  $I_l$  with experiment. As the theoretical prefactors have been adopted to the experimental  $Re/Pr^{-3/4}$  vs  $Ra$  power law, it only makes sense to check the prefactors in  $Re/Ra^{1/2}$  vs  $Pr$ . From table II the expected slope is  $-3/4$  and the expected prefactor 0.037. Linear regression gives a slope of  $-0.77 \pm 0.01$  and a prefactor of  $10^{-1.413 \pm 0.005} = 0.0386$ , cf. figure 8.

Next, we compare the experimental  $Nu$  vs  $Ra$  scaling for mercury with  $Pr = 0.025$  with theory. The measured relations  $Nu = (0.140 \pm 0.005)Ra^{0.26 \pm 0.02}$  [17],  $Nu = 0.147Ra^{0.257}$  [28], and  $Nu = 0.155Ra^{0.27}$  [15] are all in reasonable agreement with the regime  $I_l$  expectation  $Nu = 0.17Ra^{1/4}$  from table II. The same holds for a comparison in regime  $II_l$ : The reported experimental fit is  $Nu = 0.44 \pm 0.015Ra^{0.20 \pm 0.02}$  [17], theory gives  $Nu = 0.46Ra^{1/5}$ , again, remarkable agreement of both the power law exponent *and* the prefactor. Remember that the only experimental input from this experiment into the theory is  $Ra_{trans}^{I_l-II_l} = 4.5 \cdot 10^8$ .

Let us also check the prefactors of  $Nu$  as a function of  $Pr$  for fixed  $Ra = 10^6$ . A power law fit to all available experimental data points [17, 29] included in figure 2 gives  $Nu = (7.8 \pm 0.5)Pr^{0.13 \pm 0.02}$  which is in agreement with the theoretical expectation  $Nu = 0.27Ra^{1/4}Pr^{1/8} = 8.5Pr^{1/8}$  in regime  $I_l$ . Leaving out the data points for water ( $Pr = 7$ ) which strictly speaking already belongs to regime  $I_u$  gives a slightly larger power law

exponent and a slightly larger prefactor,  $Nu = 8.7Pr^{0.16}$ . Both exponent and prefactor are consistent with the theoretical expectation.

### C. Widths of the boundary layers

As stated above, the present theory also gives the absolute widths of the thermal and the laminar viscous boundary layers,

$$\lambda_\theta = 0.5LNU^{-1}, \quad (69)$$

$$\lambda_u = 0.25LRe^{-1/2}. \quad (70)$$

The results for the widths of the BLs for  $Pr = 0.025$  (mercury) and  $Pr = 7.0$  (water) are shown in figure 9. In both cases there are three regimes involved, namely,  $I_l$ ,  $II_l$ , and  $IV_l$  for  $Pr = 0.025$  and  $I_u$ ,  $III_u$ , and  $IV_u$  for  $Pr = 7.0$ . As expected, for the larger  $Pr$  numbers the thermal boundary layer is always nested in the viscous one which agrees with the experimental observations [27]. For the lower  $Pr$  numbers it is the other way round.

If the laminar BL becomes turbulent, the Blasius estimate  $\lambda_u \sim LRe^{-1/2}$  for its width must be replaced by the thickness of the turbulent BL. To give an idea about this length scale, we calculate the width  $y_0$  of the viscous sublayer of the turbulent BL within the Prandtl theory [47], applied to Couette flow. In the large  $Re$  limit it holds [47, 65]

$$\frac{y_0}{L} = 1.38 \frac{\log(k^2 Re)}{k^2 Re}. \quad (71)$$

Here,  $k = 0.4$  is the experimentally known van Kármán constant. We have included  $y_0/L$  in figure 9 for the relevant large  $Ra$ . The turbulent viscous sublayer is thinner than the laminar BL. One also notes that for the larger Prandtl number  $Pr = 7$  (water) Shraiman and Siggia's assumption [25] of the thermal boundary layer being nested in the turbulent one is just fulfilled. For lower  $Pr$  this is not the case any more.

Many experiments justify the identification of the thermal BL width with the inverse Nusselt number,  $\lambda_\theta = 0.5LNU^{-1}$ . For a detailed discussion we refer to the review articles or to Belmonte et al. [27] or to the more recent work by Lui and Xia [22].

The situation is more complicated for the width of the kinetic BL  $\lambda_u$ . Its measurement is experimentally difficult. Moreover, experimental results on  $\lambda_u$  seem to exist only for regime I.

Belmonte et al. [27] tried to measure  $\lambda_u$  in an indirect way, namely, through the detection of a spectral cutoff frequency in gas convection which in water convection (at one  $Ra$ ) is found to have a similar dependence on the height  $z$  in the RB cell as the velocity profile  $U(z)$ . For  $Pr \approx 1$  they found  $\lambda_u \approx const$  in the regime  $2 \cdot 10^7 \leq Ra \leq 2 \cdot 10^9$  and  $\lambda_u \sim L Ra^{-0.44 \pm 0.09}$  in  $2 \cdot 10^9 \leq Ra \leq 10^{11}$ . We have no idea about the origin of the measured scaling exponents.

More recently, Xin et al. [46], Xin and Xia [66], and Qiu and Xia [20] measured the thickness of the kinetic BL in a water cell in a more direct way. They define  $\lambda_u$  as the distance from the wall at which the extrapolation of the linear part of the velocity profile  $U(z)$  equals the maximum velocity  $U = \max_z U(z)$ , the velocity of the large scale wind. In

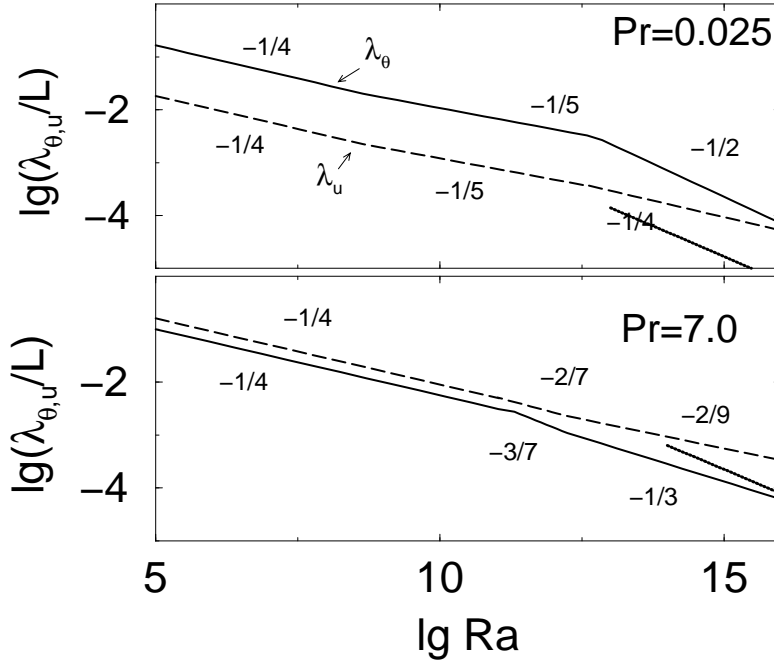


FIG. 9. Widths of the boundary layers  $\lambda_\theta = 0.5LNu^{-1}$  (solid) and  $\lambda_u = 0.25LRe^{-1/2}$  (dashed) for mercury ( $Pr = 0.025$ , upper) and water ( $Pr = 7.0$ , lower). The dotted lines show the thicknesses  $y_0$  of the viscous sublayers of a turbulent boundary layers, calculated according to eq. (71). Such a width is expected beyond the nonnormal-nonlinear transition to turbulence of the laminar shear BL (cf. section II-F).

the interval  $2 \cdot 10^8 \leq Ra \leq 10^{10}$  they find  $\lambda_u \sim LRa^{-0.16 \pm 0.02}$  for the thickness of the top and bottom kinetic BL [46, 66] and  $\lambda_u \sim LRa^{-0.26 \pm 0.03}$  for the thickness of the kinetic BLs at the side walls [20]. The first exponent (for the top and the bottom plates) is different from the value of this theory  $\lambda_u \sim LRa^{-1/4}$ . We can only speculate on the origin of this discrepancy. Perhaps, if  $\lambda_u$  is defined as the distance of the velocity maximum to the wall, the  $Ra$ -scaling would be different. The power law for the thickness of the kinetic BLs at the side walls, however, is well in agreement with the expectation  $\lambda_u \sim LRa^{-1/4}$ .

In any case, the experimentally found very weak dependence of  $\lambda_u$  on  $Ra$  supports the assumed *laminar* nature of the kinetic BL. If the width of the BL were identified with the width  $y_0$  of the viscous sublayer of a *turbulent* BL, one would expect a stronger dependence on  $Re$ , namely  $y_0 \sim L \log(k^2 Re)/(k^2 Re)$  [47, 65], i.e., when neglecting logarithmic corrections, one would have  $y_0 \sim L/Re \sim LRa^{-1/2}$ .

## D. Experimental evidence for the turbulence onset in the BL

According to the presented theory with the chosen prefactors the breakdown of laminarity in the shear BL happens at  $Ra_{turb} \approx 10^{16}$  for  $Pr = 1$  and  $Ra_{turb} \approx 10^{14}$  for  $Pr = 0.025$ . These values are calculated from table III. Hitherto, there are no experiments for these regimes.

However, one may want to argue that the transition to a turbulent shear BL may already occur earlier, be it because of a different aspect ratio, or, in view of more recent work [67, 68], because the critical Reynolds number (which we had assumed to be 420, cf. eq. (52)) is smaller, or because of a different choice of the experimental input information to which the prefactors of the theory are adopted. E.g., if one assumes a laminar shear layer with width  $\lambda_u = 1.72L/\sqrt{Re}$  as suggested by Landau and Lifshitz (ref. [47], section 39) for the (related) case of a flat plate shear flow, the transition to turbulence in the shear BL already occurs at  $Ra_{turb} = 10^{13}$  (for  $Pr = 4$ ). We note that this is just at about that  $Ra$  number where a marked transition in the (thermal) dissipative spectral power has been measured by a probe placed in the BL [7]. This transition was towards a weaker increase with  $Ra$ .

In the context of this section we also interpret the above mentioned recent experiment by Ciliberto et al. [33] in which the boundary layers are disturbed by constructing a rough bottom plate with a mean roughness comparable to the thermal boundary layer thickness. The experiments are performed in water. According to the theory of this paper one would expect larger bulk contributions to both the thermal and the kinetic dissipation and therefore an earlier onset of regime  $III'_u$  and  $IV'_u$ . Indeed, experimentally the increase of  $Nu$  with  $Ra$  is found to be much steeper. For the experiment described by Ciliberto et al. [33] the data can be fitted to power laws  $Nu \sim Ra^{0.35}$  or  $Nu \sim Ra^{0.45}$ , depending on the features of the rough bottom and upper plate.

## V. SUMMARY AND CONCLUSIONS

We summarize the central ingredients of the theory presented in this paper: The scaling laws for the Nusselt number and the Reynolds number are based on the decomposition of the global thermal and kinetic energy dissipation rates into their BL and bulk contributions. These in turn are estimated from the dynamical equations, taking the wind  $U$  as the relevant velocity in the heat conduction cell. The resulting estimates are inserted into the rigorous relations eqs. (11) and (12) for the global kinetic and thermal energy dissipation, respectively. Four regimes arise, depending on whether the bulk or the BL contributions dominate the two global dissipations. Each of the four regimes in principle divides into two subregimes, depending on whether the thermal BL (of width  $\lambda_\theta$ ) or the kinetic BL (of width  $\lambda_u$ ) is more extended.

In addition to these main regimes there is a range for very large  $Pr$  numbers in which the wind Reynolds number is  $\leq 50$ ; here the whole flow is viscosity dominated, and the theory loses its applicability. There also is the range of very small  $Pr$  numbers in which the  $Nu$  goes down to  $Nu = 1$ , and again the theory no longer holds. Finally, for large  $Ra$  the laminar kinetic BL becomes turbulent. Beyond turbulence onset we feel the flow is bulk dominated.

All scaling exponents follow from this theory. If one in addition introduces only four pieces of experimental information, also all the prefactors can be determined. Therefore the theory has predictive power not only for the power law exponents but also for the prefactors. These, however, depend on the chosen experimental information input. To nail the prefactors more input information for various aspect ratios is necessary.

The phase diagram of the theory, the main result of this work, is shown in figure 1. The power laws with the prefactors based on the chosen experimental information are summarized in table II, the power laws of the boundaries between the different regimes in table III.

A detailed comparison of the theoretical power law exponents *and* the prefactors with the experimental data gives reasonable and encouraging agreement. We emphasize that to accurately account for the dependences of  $Nu$  and  $Re$  on  $Ra$  and  $Pr$  single power laws are often not sufficient, as additive corrections from neighboring regimes can be considerable. This can be viewed as one of the main insights obtained in this paper. A particularly striking example is that  $Nu = 0.27Ra^{1/4} + 0.038Ra^{1/3}$  mimicks a  $2/7$  power law scaling over at least *nine* order of magnitude in  $Ra$ , see figure 3.

The theory also offers a possible explanation why a transition to a steeper increase of  $Nu$  vs  $Ra$  is seen in the Chavanne et al. data [19], but not in the Chicago group data [4, 6, 7]. It may be that in the large  $Ra$  Chicago experiments the  $Pr$  number was smaller than in the Chavanne et al. [19] measurements. Then for the Chicago data one had to expect a transition towards regime  $IV_u$  where the  $Ra$  scaling exponent is  $1/3$  and thus, as demonstrated, in superposition with the leading  $1/4$  exponent, is indistinguishable from a  $2/7$  scaling. In the Chavanne et al. [19] experiments, on the other hand, one has the transition to the large  $Pr$  number regime  $III_u$  where the  $Ra$  scaling exponent is  $3/7$  which is much better distinguishable from  $1/4$ . Whether this explanation is true remains to be seen.

Finally, we want to stress and discuss one of the basic assumptions of the theory, namely, that a large scale “wind of turbulence” exists, defining the Reynolds number  $Re = UL/\nu$ , creating a shear BL and stirring the turbulence in the bulk. Clearly, this assumption breaks down in the shaded area in figure 1 beyond the line  $Re = 50$  where the flow is viscosity dominated. But even below this line we do not exclude that the convection rolls break down and that the heat is exclusively transported by the fluctuations. E.g., for a water cell ( $Pr \approx 7$ ) Tanaka and Miyata [31] do not note the wind of turbulence, in contrast to Zocchi et al. [43], who do observe the wind of turbulence in their experiment with only a slightly lower aspect ratio. Also all latest experiments with various aspect ratios doubtlessly detect the wind of turbulence [20, 22, 27, 46] whose existence we therefore consider as a weak – and in particular controllable – assumption.

The present theory does *not* make any statement *how* the heat is transported from the bottom to the top, i.e., whether it is mainly convective transport or mainly transport through plumes [27]. Both processes may contribute, as both create thermal and viscous dissipation.

For even larger Prandtl numbers  $Pr \gg 7$ , the spontaneous formation of a wind of turbulence may seem more and more unlikely. To initiate such a wind so that the presented theory can be applied and results can be compared we suggest to slightly tilt the RB cell, thus breaking the symmetry and creating a preferred direction for the wind of turbulence. If this wind of turbulence can be created, we are confident that the suggested theory holds. Presently, we do not have any experimental information which contradicts the theory. How-

ever, for further verification more experiments will be valuable.

Clearly, this paper will not bring the turbulent RB heat conduction problem to an end. But we hope that the presented new approach will restimulate the discussion.

**Acknowledgments:** D. L. gratefully acknowledges S. Ciliberto's hospitality during his visit in Lyon. It was him who renewed our interest in Rayleigh-Benard convection. We thank him and S. Cioni and X. Chavanne for various discussions and also for supplying us with their experimental data and allowing us to reproduce them. We also thank G. de Bruin, L. Kadanoff, V. Steinberg, and A. Tilgner for hints and discussions. – Support for this work by the Deutsche Forschungsgemeinschaft (DFG) under the grant Lo 556/3-1, by the German-Israeli Foundation (GIF), and by the Chicago MRSEC-grant is also acknowledged. This work is part of the research programme of the “Stichting voor Fundamenteel Onderzoek der Materie (FOM)”, which is financially supported by the “Nederlandse Organisatie voor Wetenschappelijk Onderzoek (NWO)”.

e-mail addresses:

grossmann@physik.uni-marburg.de

lohse@tn.utwente.nl

- 
- [1] A. H. Davis, *Phil. Mag.* **43**, 329 (1922); *Phil. Mag.* **44**, 920 (1922).
  - [2] M. V. R. Malkus, *Proc. R. Soc. London A* **225**, 196 (1954).
  - [3] F. Heslot, B. Castaing, and A. Libchaber, *Phys. Rev. A* **36**, 5870 (1987).
  - [4] B. Castaing *et al.*, *J. Fluid Mech.* **204**, 1 (1989).
  - [5] T. H. Solomon and J. P. Gollub, *Phys. Rev. Lett.* **64**, 2382 (1990).
  - [6] X. Z. Wu and A. Libchaber, *Phys. Rev. A* **43**, 2833 (1991).
  - [7] I. Procaccia *et al.*, *Phys. Rev. A* **44**, 8091 (1991).
  - [8] J. Werne, *Phys. Rev. E* **48**, 1020 (1993).
  - [9] F. Chilla, S. Ciliberto, C. Innocenti, and E. Pampaloni, *Il Nuovo Cimento D* **15**, 1229 (1993).
  - [10] E. D. Siggia, *Annu. Rev. Fluid Mech.* **26**, 137 (1994).
  - [11] S. Cioni, S. Ciliberto, and J. Sommeria, *Europhys. Lett.* **32**, 413 (1995).
  - [12] E. Villermaux, *Phys. Rev. Lett.* **75**, 4618 (1995).
  - [13] R. Kerr, *J. Fluid Mech.* **310**, 139 (1996).
  - [14] Y. Shen, P. Tong, and K. Q. Xia, *Phys. Rev. Lett.* **76**, 908 (1996).
  - [15] T. Takeshita, T. Segawa, J. A. Glazier, and M. Sano, *Phys. Rev. Lett.* **76**, 1465 (1996).
  - [16] S. Ciliberto, S. Cioni, and C. Laroche, *Phys. Rev. E* **54**, R5901 (1996).
  - [17] S. Cioni, S. Ciliberto, and J. Sommeria, *J. Fluid Mech.* **335**, 111 (1997).
  - [18] K.-Q. Xia and S.-L. Lui, *Phys. Rev. Lett.* **79**, 5006 (1997).
  - [19] X. Chavanne *et al.*, *Phys. Rev. Lett.* **79**, 3648 (1997).
  - [20] X. L. Qiu and K.-Q. Xia, *Phys. Rev. E* **58**, 486 (1998).

- [21] Y. B. Du and P. Tong, Phys. Rev. Lett. **81**, 987 (1998).
- [22] S. L. Lui and K. Q. Xia, Phys. Rev. E **57**, 5494 (1998).
- [23] R. Benzi, F. Toschi, and R. Tripiccion, J. Stat. Phys. **93**, 901 (1998).
- [24] S. Zaleski, in *Geophysical and Astrophysical Convection*, edited by P. Fox and R. Kerr (Gordon and Breach Science Publishers, New York, 1998).
- [25] B. I. Shraiman and E. D. Siggia, Phys. Rev. A **42**, 3650 (1990).
- [26] E. S. C. Ching, Phys. Rev. E **55**, 1189 (1997).
- [27] A. Belmonte, A. Tilgner, and A. Libchaber, Phys. Rev. E **50**, 269 (1994).
- [28] H. T. Rossby, J. Fluid Mech. **36**, 309 (1969).
- [29] S. Horanyi, L. Krebs, and U. Müller, Int. J. of Heat Mass Transfer (1999).
- [30] A. M. Garon and R. J. Goldstein, Phys. Fluids **16**, 1818 (1973).
- [31] H. Tanaka and H. Miyata, Int. J. Heat Mass Transfer **23**, 1273 (1980).
- [32] R. J. Goldstein and S. Tokuda, Int. J. of Heat Mass Transfer **23**, 738 (1980).
- [33] S. Ciliberto and C. Laroche, Phys. Rev. Lett. **82**, 3998 (1999).
- [34] S. Ashkenazi and V. Steinberg, Phys. Rev. Lett., submitted 1999, chao-dyn/9903021.
- [35] D. C. Threlfall, J. Fluid Mech. **67**, 17 (1975).
- [36] J. A. Glazier, T. Segawa, A. Naert, and M. Sano, Nature **398**, 307 (1999).
- [37] R. H. Kraichnan, Phys. Fluids **5**, 1374 (1962).
- [38] X. Z. Wu, Ph.D. thesis, University of Chicago, 1991.
- [39] L. N. Howard, Ann. Rev. Fluid. Mech. **4**, 473 (1972).
- [40] F. H. Busse, Adv. Appl. Mech. **18**, 77 (1978).
- [41] C. Doering and P. Constantin, Phys. Rev. E **53**, 5957 (1996).
- [42] R. Krishnamurti and L. N. Howard, Proc. Natl. Acad. Sci. **78**, 1981 (1981).
- [43] G. Zocchi, E. Moses, and A. Libchaber, Physica A **166**, 387 (1990).
- [44] A. Belmonte, A. Tilgner, and A. Libchaber, Phys. Rev. Lett. **70**, 4067 (1993).
- [45] A. Tilgner, A. Belmonte, and A. Libchaber, Phys. Rev. E **47**, 2253 (1993).
- [46] Y. B. Xin, K. Q. Xia, and P. Tong, Phys. Rev. Lett. **77**, 1266 (1996).
- [47] L. D. Landau and E. M. Lifshitz, *Fluid Mechanics* (Pergamon Press, Oxford, 1987).
- [48] D. P. Lathrop, J. Fineberg, and H. S. Swinney, Phys. Rev. Lett. **68**, 1515 (1992).
- [49] S. Grossmann, Phys. Rev. E **51**, 6275 (1995).
- [50] E. A. Spiegel, Ann. Rev. Astron. Astrophys. **9**, 323 (1971).
- [51] S. K. Chan, Stud. Appl. Math. **50**, 13 (1971).
- [52] P. Constantin and C. Doering, J. Stat. Phys. **94**, 159 (1999).
- [53] G. O. Roberts, Geophys. Astrophys. Fluid Dyn. **12**, 235 (1979).
- [54] T. E. Faber, *Fluid Dynamics for Physicists* (Cambridge University Press, Cambridge, 1995).
- [55] R. M. Clever and F. H. Busse, J. Fluid Mech. **102**, 61 (1981).
- [56] F. H. Busse and R. M. Clever, J. Fluid Mech. **102**, 75 (1981).
- [57] P. Drazin and W. H. Reid, *Hydrodynamic stability* (Cambridge University Press, Cambridge, 1981).
- [58] L. Boberg and U. Brosa, Z. Naturforsch. **43a**, 696 (1988).
- [59] L. Trefethen, A. Trefethen, S. Reddy, and T. Driscoll, Science **261**, 578 (1993).
- [60] T. Gebhardt and S. Grossmann, Phys. Rev. E **50**, 3705 (1994).
- [61] F. Waleffe, Phys. Fluids **7**, 3060 (1995).
- [62] A. Schmiegel and B. Eckhardt, Phys. Rev. Lett. **79**, 5250 (1997).
- [63] S. Grossmann, "The onset of shear flow turbulence", Rev. Mod. Phys., submitted 1999.



- [64] V. Yakhot, Phys. Rev. Lett. **69**, 769 (1992).
- [65] unpublished material (unpublished).
- [66] Y. B. Xin and K. Q. Xia, Phys. Rev. E **56**, 3010 (1997).
- [67] B. Eckhardt and A. Mersmann, Phys. Rev. E **60**, 509 (1999).
- [68] A. Schmiegel and B. Eckhardt, “Dynamics of perturbations in plane Couette flow”, preprint, Marburg 1999.